AIR FORCE INSTITUTE OF TECHNOLOGY

AIR UNIVERSITY
UNITED STATES AIR FORCE

SCHOOL OF ENGINEERING

WRIGHT–PATTERSON AIR FORCE BASE, OHIO

AF-WP-O-MAY 62 3,500

ENERGY BALANCE OF A WHIRL STABILIZED HYDROGEN ARC

Capt Thomas E. Reinhardt

GNE/Phys/62-15

ENERGY BALANCE OF A WHIRL STABILIZED HYDROGEN ARC

THESIS

Presented to the Faculty of the School of Engineering of
the Air Force Institute of Technology
Air University
in Partial Fulfillment of the
Requirements for the Degree of
Master of Science

By
Thomas E. Reinhardt, B.S. Mil. Sc.
Capt USAF

Graduate Nuclear Engineering
July 1962

Preface

This report is written so that you can skip Chapter II, Apparatus; Chapter III, Experimentation; and Chapter IV, Data without loss of continuity. I apologize to the diligent reader for the repetition which follows from such a construction.

I am very grateful to Mr. Paul Schrieber for the many hours he generously spent calibrating the radiometer and for the accompanying short course in optics. I would like to express my appreciation for the wonderful cooperation which I received from all the members of the Aeronautical Research Laboratory, my wife, and my excellent typist.

Contents

Contents

List of Figures

Abstract

A whirl stabilized hydrogen arc existed in a transparent vycor tube between flat copper electrodes, each having axial gas discharge holes. The purpose of this investigation was to make an energy balance on this arc by the method of water calorimetry. The total energy balance revealed questionable stability below ninety amperes. A marked hysteresis was observed between sixty and ninety amperes by varying chamber pressure. The initial increase of power at constant pressure led to a positive voltage-current characteristic. Enthalpy ranged from 30,000 to 70,000 BTU/lb. Efficiency varied from eighty to ninety percent. Electrode losses were optimized by decreasing the cathode discharge hole diameter. Suggestions for improvements leading to higher enthalpy, stability, and lifetime are included.

ENERGY BALANCE OF A WHIRL STABILIZED HYDROGEN ARC

I. Introduction

General

Electrical discharges in gases have been pre-eminent in the development of modern science both as a tool and as a basic physical phenomena. Myriad applications have resulted from the countless investigations which have been undertaken. Sodium vapour lamps, neon tubes, rectifiers, welding arcs, hypersonic wind tunnels, and hopefully thermonuclear reactors are just a few examples.

Although over two-hundred years of serious investigation has elapsed since Franklin's celebrated kites, knowledge of the electric arc is still incomplete. A uniform and complete theoretical description of the mechanisms for the several arc types is not available. Even in some of the simplest direct current arcs, certain aspects such as the cathode fall region are not completely understood. For this reason, arc operation and development must be based at least in part on empirical data.

The last two of the examples cited above are quite modern applications of a well-known aspect of electric arcs. The high temperatures associated with electric arcs have been used for cutting, welding, and coating metals for some time. The case of a hypersonic

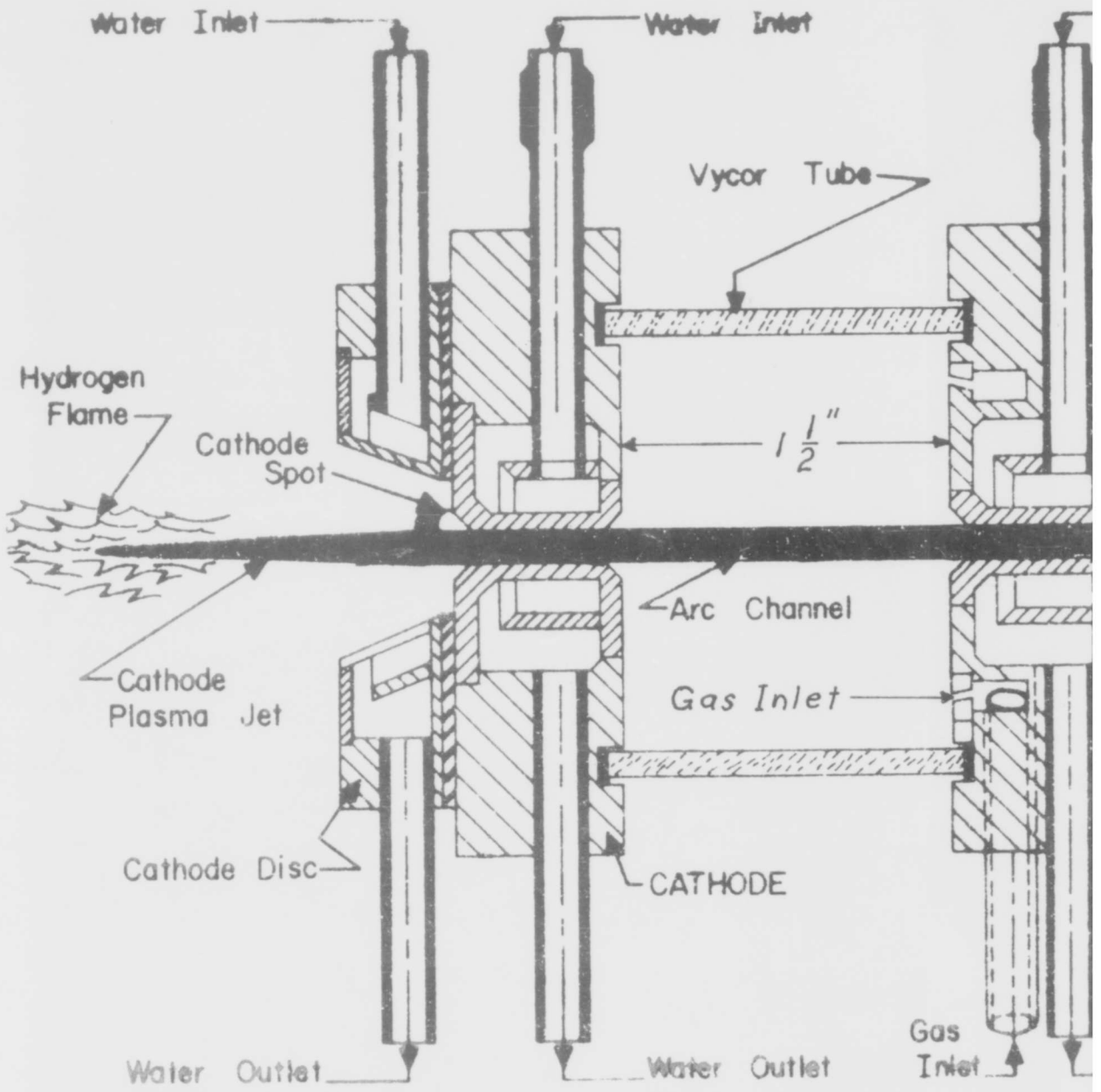

Figure 1

Schematic Cross-Section of the Hydrogen Arc Chamber

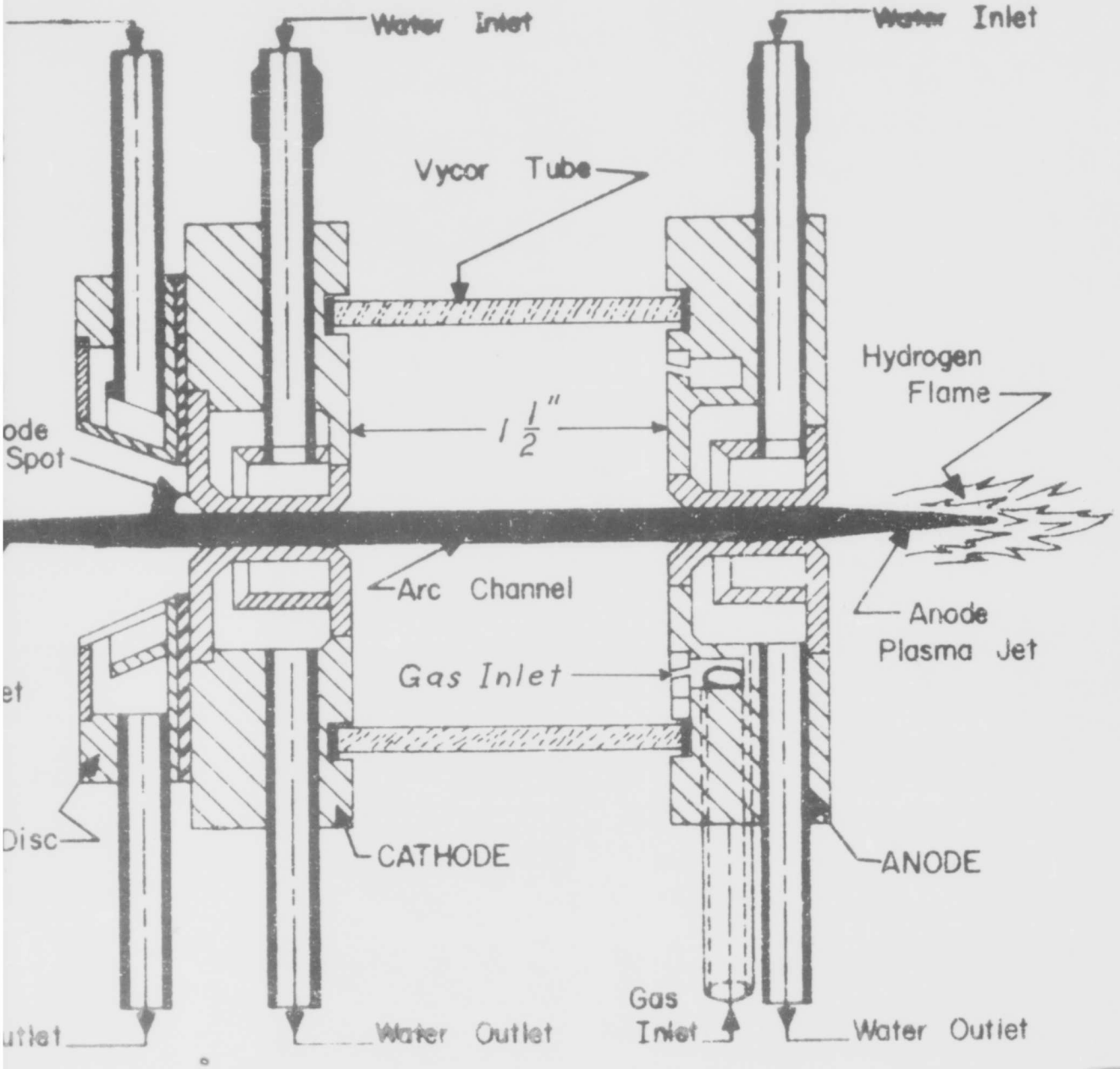

Figure 1

Schematic Cross-Section of the Hydrogen Arc Chamber

2

wind tunnel is merely an extension of the role of the arc as a heater. For this purpose the important considerations are efficiency and high specific enthalpy. The lifetime of the apparatus can also be important.

Thermonuclear reactions or, to be a little less presumptuous, plasma physics theoretical studies make use of the high temperature aspect of electric arcs also. In this case, the arc is only the beginning of a process for achieving extremely high temperatures and perhaps a self-sustaining reaction. This beginning is an important step in itself and such considerations as stability, reproduceability, ease of analysis, and high peak temperature are of interest. Efficiency and lifetime play a secondary role in this example; however, a knowledge of them is important to the operation of an experiment.

Description of the Arc

Physical Description. One excellent device for such theoretical studies is the whirl-stabilized hydrogen arc shown schematically in Figure 1. The discharge chamber is a transparent vycor tube sealed at the ends by flat, cylindrical, water-cooled, copper electrodes. The gas enters the chamber through six holes in the anode and exits through axial holes in each electrode. The inlet holes in the anode are drilled at an angle which gives a tangential velocity to the gas. This creates a vortex with a consequent decrease in pressure near the axis accompanied by strong cooling in this region. This cooling and rarefaction causes constriction and space stabilization of the arc along the axis.

The water-cooled, electrically insulated disk mounted on the cathode, is at a floating potential and prevents the arc from jumping to the region of high field intensity at the outside corner of electrode.

Theory of Operation. Assuming constant geometry, the indepentent variables for this arc are electric current and gas supply pressure. Fixing these two will determine voltage, power, gas flow rate, enthalpy, peak temperature, arc diameter, and radiation. At constant current, an increase in pressure will cause the voltage, power, mass flow rate, peak temperature and radiation to increase. Enthalpy and arc diameter will decrease.

At constant pressure an increase in current will result in an increase of power, enthalpy, peak temperature, and radiation losses. Gas flow rate will not change significantly and arc diameter will increase only slightly, if at all, for small (less than ten percent) changes of current. Voltage will decrease for an increase of current at constant pressure because of the increase in conductivity. Conductivity increases with temperature within the operating range of this arc and temperature increases with current. The reason voltage increases with increased pressure at constant current is the decrease in arc diameter. This has a more pronounced effect than the associated axial temperature increase.

Several qualifications must be imposed on the above description which applies in general only to the column and not to the anode and cathode fall regions. Most important and least understood are changes in geometry of the discharge holes due to melting and sputtering,

especially at the cathode. This gradual increase in hole diameter during operation changes the radial pressure gradient near the arc column and increases the flow rate for a given supply pressure. For this investigation preliminary analysis showed mass flow rate to be a better parameter than pressure for graphical presentation. Shapes of curves did not alter between using pressure or flow rate as a parameter but using flow rate gave less dispersion of data points. The probable reason for this dependence is the gradual increase in hole diameter.

Another qualification is that during normal operation the exit conditions do not vary except as regards the changing diameter of the discharge holes. However, the apparatus used during this experiment made possible variation of the ambient pressure at the outside of the anode. This in turn affected the proportion of the mass flow out either end of the chamber and therefore gas velocity and, most important, electrode losses.

The last qualification is with respect to the voltage increase at constant current due to increased pressure. Part of this increased voltage is believed due to the necessity for the arc to penetrate the sheath of cold gas which separates it from the electrodes, this sheath being colder and thicker at higher flow rates. This effect should be greater at the cathode than at the anode if electrons and ions are the charge carriers in the anode fall and cathode fall respectively.

It should be emphasized that the explanation of the negative characteristic given above applies only to the arc column. The characteristic curves obtained from this investigation were for the total energy balance and thus include anode fall, cathode fall and ohmic heating. Therefore, the presence of a positive segment of these characteristic curves does not necessarily conflict with theory.

The Problem. The whirl-stabilized hydrogen arc is the subject of this investigation which seeks information about reproduceability, efficiency, and enthalpy. The investigation will also yield information about arc operating techniques and electrode loss mechanisms. Concurrent photographic and spectroscopic studies, which will be published elsewhere, seek information about stability, temperature profiles, and peak temperature.

The method of this investigation is a total energy balance. Theoretical treatment of this method is hampered by incomplete knowledge of the electrode loss mechanisms, especially at the cathode. The instability of the cathode spot in this particular device also causes difficulty in the interpretation of experimental results.

The problem stated in detail is: (1) Measure the electrical energy input to the arc, (2) Measure the amount of energy lost to the electrodes, (3) Measure the amount radiated away through the vycor tube, (4) Measure the amount carried away by the gas as it flows out the axial holes in the electrodes. A small amount of energy comes out the axial holes in the form of radiation. This radiation should

be determined and, if significant, subtracted from the amount carried away by the gas.

With the exception of the energy radiated out the axial holes, all losses were measured by water calorimetry. For steady state conditions the expression is:

$$Q = MC_p (T_{out} - T_{in}) \qquad (1)$$

Axial radiation was measured with a circular foil radiometer.

Figure 2

Total Radiation Calcrimeter, Anode Removed

II. Apparatus

Electrical Power Measurement

The input electrical power was measured with standard direct current instruments. A Weston Model 1 millivoltmeter (0-200 mv) was employed with a two hundred ampere, fifty millivolt precision shunt to measure current. A Universal Polyranger Model U voltmeter (0-1000 v) was used to measure supply voltage. Current and voltage were recorded on a two-channel Brown Potentiometer Model BY 153X in addition to the other two instruments.

Electrode Power Loss Measurement

The electrode losses were measured by recording inlet and outlet water temperatures. Chrome-Alumel thermocouples were used here and in the remaining water temperature measurements. The thermocouple outputs were recorded on a twelve-channel Honeywell Visicorder Model 906B. Water temperatures in the electrode system remained below thirty degrees centigrade so that radiation and free-convection cooling were not significant. The electrodes were nickel-plated and polished to reduce the absorbtion of radiation from the arc. In the ultra-violet range, the reflectivities are about thirty percent and fifty percent for polished copper and polished nickel respectively. At longer wavelengths, the reflectivity of nickel is similar to that of copper. (Ref. 5; 2950)

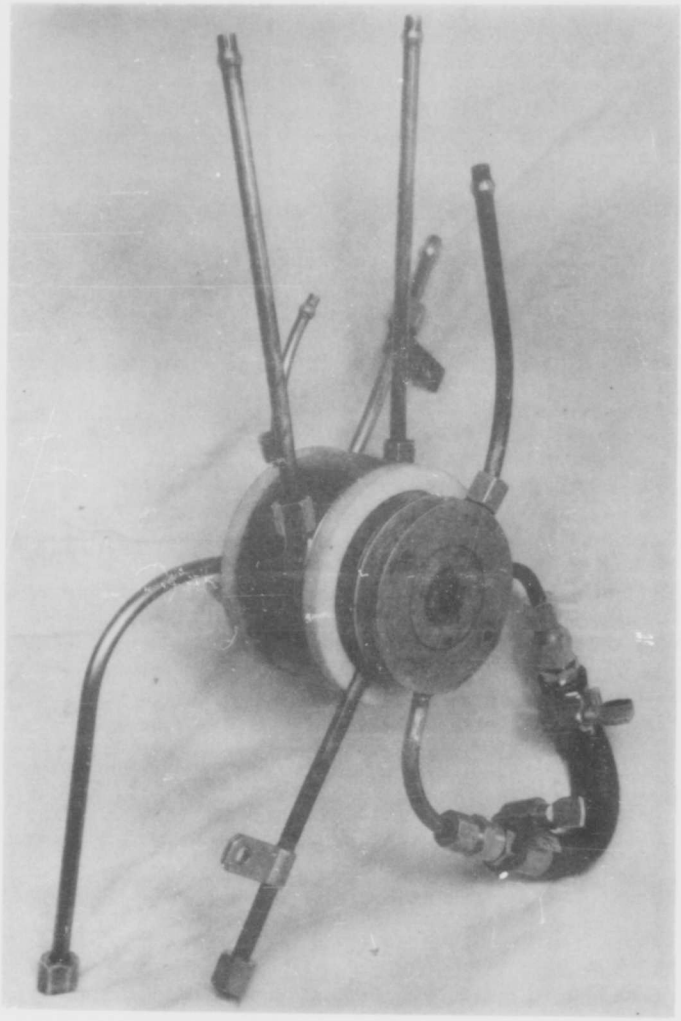

Figure 3

Total Radiation Calorimeter Between Electrodes

Radial Radiation Loss Measurement

The radiation loss through the vycor tube was measured with a total-radiation, copper calorimeter (Figure 2) which was fabricated in the laboratory. Figure 3 shows the radiation calorimeter assembled between the electrodes. This calorimeter completely surrounded the vycor tube and was insulated from the electrodes by teflon rings. When assembled only a one-eighth inch lip of each teflon ring was exposed to the arc. The remaining exposed surfaces were the polished electrode faces and the inner surface of the calorimeter. This surface was painted with camouflage-black lacquer (Reflectivity in the visible and near ultra-violet about six percent according to the Base Paint Shop, Building Five, Wright-Patterson Air Force Base). Water circulated behind the inner surface and the inlet and outlet temperatures were measured as in the case of the electrodes. It was found necessary to circulate air within the space between the vycor tube and the absorbing surface of the calorimeter. This circulation was caused by applying a vacuum which sucked ambient air in around the teflon rings. This heated air, after cooling the vycor tube and the black absorbing surface, passed through the cooling water of the calorimeter before leaving the system. The air outlet or suction tube was cool to the touch during operation. Thus the heat of radiation collected by this air was transferred to the water and properly recorded. The modification was made after the photographs for Figure 2 and 3 had been taken.

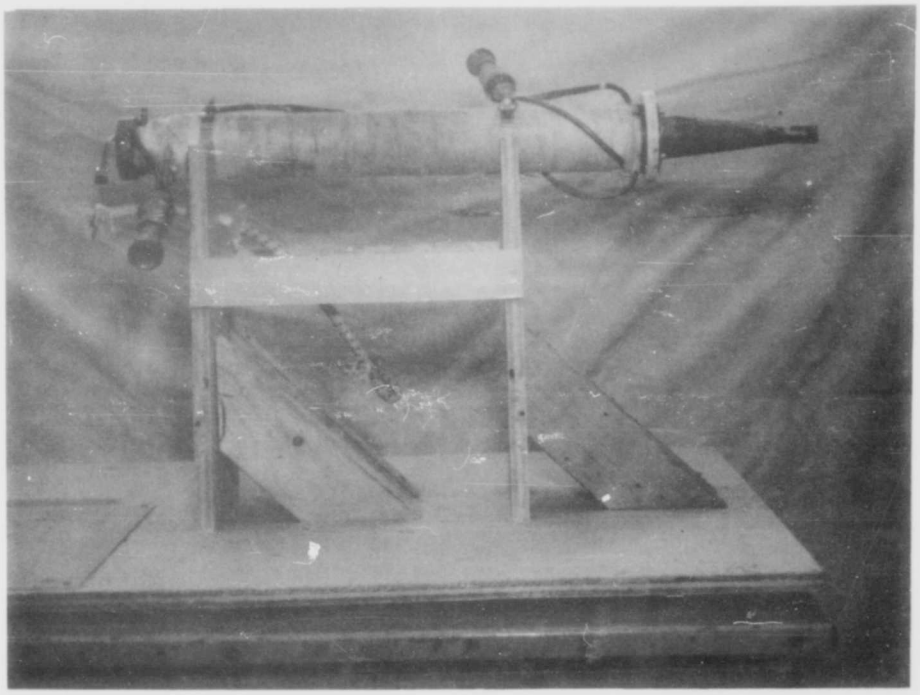

Figure 4

Heat Exchanger for Gas Convection Measurement

Figure 5

Heat Exchanger Coils

Gas Convection Measurement

The heat loss by convection and radiation out the axial holes was measured by two counterflow heat exchangers (Figure 4) designed and fabricated in the laboratory with the help of Base Shops who wrapped the co-axial cooling coils (Figure 5). These heat exchangers reduced the gas to room temperature and had a measured pressure drop of one and one half inches of water at the maximum flow rate used in this experiment. The heat exchangers were made entirely of copper and wrapped with fiberglass insulation. Water temperatures as high as 60°C were recorded so the water outlets from the heat exchangers were well insulated to prevent re-radiation and convective cooling.

Axial Radiation Loss

The axial radiation was measured with a circular foil radiometer (CFR-1A) made by Arthur C. Ruge Associates, Inc. (Ref. 4;366). The radiometer was calibrated with a National Bureau of Standards total radiation source. A level table with a one-meter arm pivoted at one end was provided to mount the radiometer. The pivot point was positioned directly below the discharge end of the axial hole in the cathode. A pointer attached to the pivoting arm indicated the position of the radiometer in the horizontal plane. The position was measured in degrees of inclination from the axis. A breeze of pressurized air provided for the deflection of the burning gas thus insuring that only radiation was recorded by the radiometer.

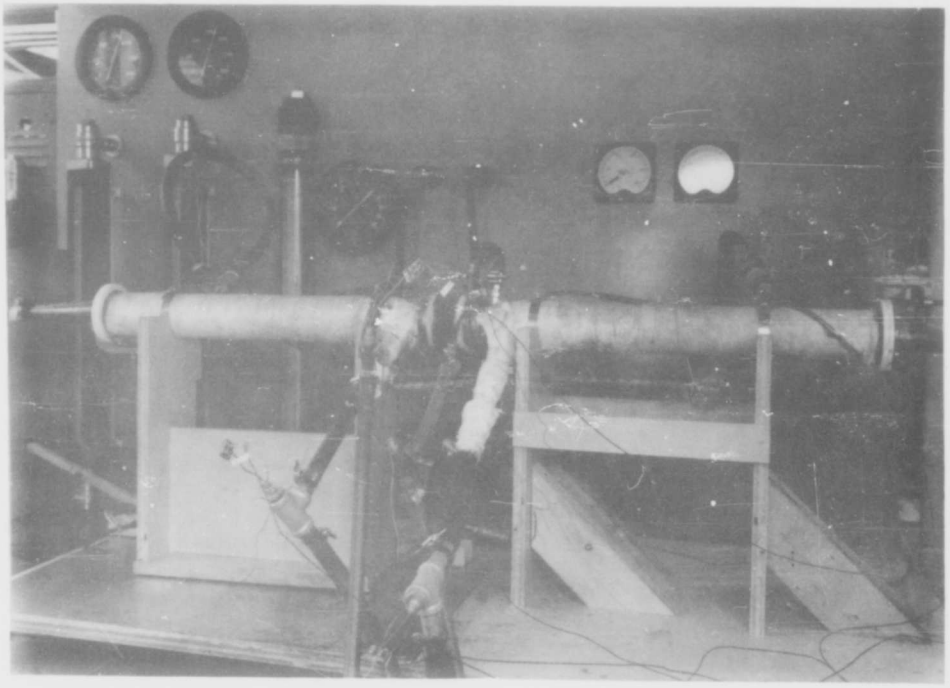

Figure 6

Original Experimental Arrangement

Gas and Water Flow

Gas and water flow rates were measured with rotameter type instruments manufactured by Fisher-Porter Company. All flowmeters were calibrated in the laboratory. The gas flowmeters were calibrated against a standard bellows-type positive displacement meter supplied by the Dayton Power and Light Company.

Inlet gas flow out of each heat-exchanger was also measured thus assuring the integrity of the experiment with respect to both mass and energy.

Modifications

Unfortunately the pressure drop across the rotameter and associated ducting downstream from the heat-exchanger was on the order of one-half p.s.i.a. This made the experiment somewhat artificial. More important, it caused the cathode spot to recede into the axial hole instead of running around on the outside face of the electrode. This caused very rapid cathode erosion and failure even at low power levels.

In spite of the rapid cathode failure rate, fifty-six tests were made with the two heat-exchanger arrangement shown in Figure 6. These tests demonstrated an extremely high degree of integrity. The total energy collected compared to the input electrical energy within two percent. The inlet gas flow compared to the total outlet gas flow within five percent. These results justified removal of the heat exchanger on the cathode side. In subsequent tests the energy and gas flow out the cathode side were determined by subtraction.

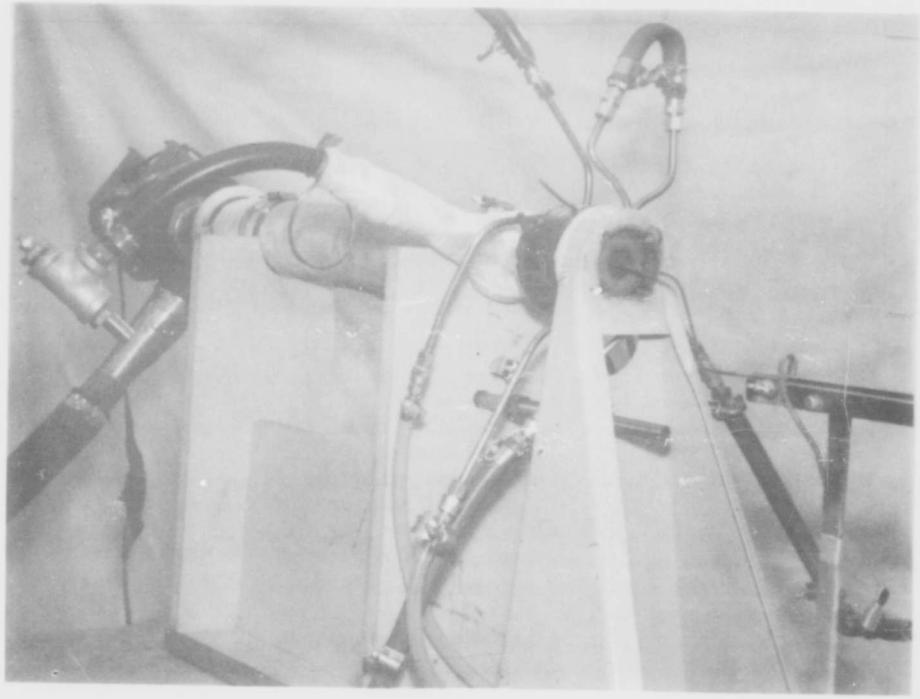

Figure 7

Modified Experimental Arrangement

In addition to removing the heat-exchanger at the cathode side, certain refinements were made at the anode side to eliminate the artificial situation mentioned above. A centrifugal fan followed by a valve was installed downstream from the anode heat-exchanger. The outlet gas rotameter was replaced by the Dayton Power and Light Company bellows-type flowmeter which had a much smaller pressure drop. A pressure probe from a mercury manometer was added at the throat of the heat-exchanger. This fan and valve arrangement allowed control of the discharge pressure at the anode side. The fan was strong enough to induce a zero p.s.i.g. discharge pressure up to a hydrogen gas flow rate of thirty-five grams per minute. At the maximum flow rate of forty-two grams per minute used during the tests, the over-pressure was less than 0.05 p.s.i.g. Thus the only deviation from discharging to atmospheric conditions, resulting from the presence of the anode heat exchanger, was the temperature and type of gas which made up the atmosphere at the anode side. The modified experimental arrangement except for the valve is shown in Figure 7.

Power Supply

The power supply consisted of two direct current rectifiers rated at two-hundred and fifty amperes, five-hundred volts continuous operation. A series resistor was employed below fifty kilowatts operating power because of the nature of the rectifier load line.

III. Experimentation

Five separate investigations were conducted. The principal investigation was the energy balance and it will be presented first. The unusual characteristic curves obtained during the energy balance investigation inspired two minor investigations. These will be presented following the description of the energy balance and conclude the investigations which actually produced data for the results of this report. Two other investigations of a diagnostic nature were conducted. They were concerned with the axial radiation loss and the integrity of the energy balance respectively. Description of these two investigations concludes the chapter.

Energy Balance

The data for the energy balance was obtained by varying supply pressure with rectifier power setting remaining constant. Actually there was some slight variation in power because of the non-linear load line of the rectifiers. A typical series of tests will be described. The only variation from series to series being the size of the increment of pressure. At low power the pressure was changed from eighteen p.s.i.g. to thirty p.s.i.g. by increments of two p.s.i.g. At high (sixty kilowatts and above) power, the pressure was changed from twenty p.s.i.g. to forty p.s.i.g. by increments of five p.s.i.g.

The anode fan was turned on for all tests and the valve was adjusted to make the anode discharge pressure equal to ambient atmospheric pressure. Fortunately the valve adjustment was overlooked on

several occasions and the consequent random variation of discharge pressure proved to be fortuitous in the dispersion of data points. It is now obvious that this parameter should have been varied methodically. However, within the given number of experiments that were made, little more information could have been gathered than was accomplished by the random variation.

A series of tests using hydrogen was conducted as follows: The discharge chamber was tested for leaks up to forty p.s.i.g. static pressure by closing the axial discharge holes. The exhaust system was checked for leaks up to three p.s.i.g. static pressure by closing the axial hole in the cathode and the exhaust valve on the anode side. Cooling water was turned on and flow rates adjusted to best accommodate the power programmed for the test series. Too low a flow rate would cause high water temperatures resulting in re-radiative and convective losses. Too high a flow rate would result in a temperature difference too small to be read accurately from the visicorder paper. Finally, the visicorder and the anode fan were turned on just prior to starting.

The arc was started in nitrogen at twenty-five p.s.i.g., then the gas was changed to hydrogen by lowering the nitrogen pressure below twenty p.s.i.g., the pre-set hydrogen pressure. Because of stagnation areas in the chamber a thirty second pause was required at this point to eliminate all nitrogen from the chamber. The time delay was determined by spectroscopical studies. During this wait the power level was increased to the predetermined level for the test series. It was important not to increase the power before changing to hydrogen since

cathode erosion was quite rapid with nitrogen at high power levels.

After thirty seconds the gas flow, water flow, current, voltage, and pressure readings were recorded and the paper in the two recorders was marked. Then the supply pressure was incremented by five p.s.i.g. per test to a maximum of forty p.s.i.g. A twenty second wait at each pressure was needed to allow for the slow response of the radiation calorimeter (time constant about four seconds). After the series of five tests the gas was changed to nitrogen and the arc immediately extinguished by opening the circuit. At low power levels with either gas, ten or fifteen tests were possible before cathode failure. At high (seventy kilowatts) power levels using hydrogen gas the cathode would last for about five tests and with nitrogen only two or three. The anode lifetime was about five times that of the cathode.

Data was taken for both hydrogen and nitrogen gas; however, the emphasis was on the hydrogen experiment. Much of the data on nitrogen was obtained during diagnostic tests of the apparatus. An attempt was made toward the end to fill in enough data points to allow an analysis but this attempt was only partially successful. Consequently the results obtained from the nitrogen tests are incomplete and of questionable validity.

Characteristics

Varying Power. The first minor investigation was for the purpose of obtaining data for a characteristic curve by varying power while keeping the pressure constant. This investigation was made without the

energy balance apparatus connected in an attempt to see if that apparatus had any influence on the characteristic curve. There was no apparent influence. The conduct of the test series was similar to that of the energy balance except that pressure was maintained at twenty-five p.s.i.g. while current was incremented from sixty-six and one-half amperes to one hundred seventy-eight amperes and back down to sixty-five amperes.

Varying Pressure. The second minor investigation was for the purpose of obtaining information about the arc characteristic as pressure varied up and down. As in the previous investigation the energy balance apparatus was not connected. The conduct of the test series was similar to that of the energy balance except that the arc was stabilized at twenty-five p.s.i.g. and then incremented down to eighteen p.s.i.g., back up to twenty-eight p.s.i.g., and finally returned to twenty-five p.s.i.g. Three test series of this type were conducted, each series with a different rectifier setting. The power did not remain constant as expected for a given rectifier setting.

Diagnostic Experiments

Axial Radiation. The axial radiation measurements were made independently from the foregoing energy balance. The arc was operated at one hundred amperes, five hundred and ninety volts, twenty p.s.i.g. supply pressure. A radiation intensity profile at one meter distance was taken between 0° and 50° inclination to the axis. Output from the meter was measured on a microvolt bridge with zero readings taken between each measurement. Asbestos shields were positioned so that

the radiometer absorbed radiation from the cathode discharge side only.

The total axial radiation at the cathode side was 0.25 kw at one hundred amps. This is similar to the amount in the radial direction at the same current and flow rate. The loss in enthalpy resulting from this radiation is less than two percent and it will be neglected. No axial radiation measurements were made with nitrogen but it is reasonable to assume that results would also correspond to the radial measurement. Neglecting the effect on enthalpy in nitrogen would thus introduce an error of four to eight percent.

Preliminary Tests. The preliminary diagnostic tests of the apparatus were conducted in exactly the same manner as the energy balance tests already described. The only difference was in the apparatus. For the diagnostic tests there was a heat-exchanger at both the cathode and anode side so that all the energy was measured. In addition, the heat-exchanger at the anode side did not have the suction fan and valve arrangement employed during the energy balance tests.

IV. Data and Calculations

This chapter is a presentation of raw (Table I) and reduced (Table II) data from the hydrogen experiment. The temperature difference information in Table I is not actually raw data, having been transformed from the thermocouple trace on the Visicorder paper by means of calibration curves. Error limits are given in Chapter V.

As an example, the information from Table I, Test No. 83 will be reduced to the results for Table II, Test No. 83.

Total Power

$$P = EI = 620\ (104) = 64.5 \text{ kw} \tag{2}$$

Radiation Loss

$$Qr = MC_p\ (T_{out} - T_{in})k = 1.48(1)(4.30)(0.000526) \tag{3}$$
$$= 0.33 \text{ kw}$$

Anode Loss

$$Q_a = 555(1)(10.95)(0.000526) = 3.20 \text{ kw} \tag{4}$$

Cathode Loss

$$Q_c = 884(1)(17.31)(0.000526) = 8.05 \text{ kw} \tag{5}$$

Anode Gas Loss

$$Q_{ag} = 1494(1)(29.8)(0.000526) = 23.5 \text{ kw} \tag{6}$$

Sub-Total

$$S = Q_r + Q_a + Q_c + Q_{ag} = 35.08 \text{ kw} \tag{7}$$

Cathode Gas Loss

$$Q_{cg} = P - S = 64.5 - 35.08 = 29.42 \text{ kw}. \tag{8}$$

Enthalpy (H) is defined

$$H = U + PV/J$$

where U for this experiment is the amount of energy collected by the heat exchanger and PV/J = 500 BTU/lb, an average value admissible because the hydrogen gas was reduced to room temperature and pressure before leaving the heat exchanger.

Total Gas Flow

M_t = 32.4 gr/min, from calibration curves

Anode Gas Flow

$$M_a = (1/12.67)60 = 4.74 \text{ ft}^3/\text{min at } 72^\circ\text{F}, 14.24 \text{ p.s.i.a.} \quad (9)$$

$$= 10.81 \text{ gr/min (by ideal gas laws)}$$

Cathode Gas Flow

$$M_c = M_t - M_a = 32.4 - 10.81 = 21.6 \text{ gr/min} \quad (10)$$

Total Enthalpy

$$H_t = (Q_{ag} + Q_{cg})k/M_t + 500 \quad (11)$$

$$= (52.92)25.79/32.4 + 500 = 42,600 \text{ BTU/lb}$$

Anode Gas Enthalpy

$$H_a = (Q_{ag})k/M_a + 500 = (23.5)25.79/10.81 + 500 \quad (12)$$

$$= 56,600 \text{ BTU/lb}$$

Cathode Gas Enthalpy

$$H_c = (Q_{cg})k/M_c + 500 = (29.42)25.79/21.6 + 500 \quad (13)$$

$$= 35,600 \text{ BTU/lb}$$

Test No.	Pressure in PSIG	Current in Amperes ÷ 4	Voltage in Volts	Inlet Gas Flow in Scale Units	Outlet Gas Flow	
					FT^3	Sec
73	18	26	520	29.4	1.0	15.48
74	20	24	555	32.3	1.0	14.90
75	22	22	590	34.5	0.7	9.70
76	24	20	610	36.4	1.0	13.54
77	24	25	599	36.2	1.0	14.17
78	20	27	550	33.3	1.0	16.41

Test No.	Water Flow in LB/HR				Water Temperature Difference in °C			
	Radiation	Anode	Cathode	Anode Gas	Radiation	Anode	Cathode	Anode Gas
73	150	555	889	1507	4.42	12.41	8.78	26.3
74	150	555	884	1507	3.4	10.71	8.54	25.2
75	150	555	889	1507	3.2	9.74	8.54	24.9
76	150	555	889	1507	2.8	8.53	9.27	24.9
77	150	555	889	1509	3.8	10.93	11.71	27.0
78	150	555	889	1512	4.3	12.16	12.31	25.6

TABLE I.
TOTAL ENERGY BALANCE, RAW DATA

Test No.	Pressure in PSIG	Current in Amperes ÷4	Voltage in Volts	Inlet Gas Flow in Scale Units	Outlet Gas Flow	
					FT^3	Sec
79	28	22	650	39.5	1.0	13.95
80	32	20	680	41.8	1.0	11.66
81	20	31	515	34.5	1.0	17.31
82	25	28	572	37.8	1.0	14.88
83	30	26	620	41.0	1.0	12.67
84	35	24	650	43.8	1.0	11.18

Test No.	Water Flow in LB/HR				Water Temperature Difference in °C			
	Radiation	Anode	Cathode	Anode Gas	Radiation	Anode	Cathode	Anode Gas
79	150	555	889	1512	3.2	9.02	12.20	25.1
80	150	555	889	1512	2.83	7.55	12.31	23.7
81	148	550	884	1497	5.1	14.61	19.27	27.2
82	148	555	884	1494	4.52	13.14	19.02	28.7
83	148	555	884	1494	4.3	10.95	17.31	29.8
84	148	555	884	1494	3.85	9.75	15.86	29.4

TABLE I. CONT.

TOTAL ENERGY BALANCE, RAW DATA

Test No.	Pressure in PSIG	Current in Amperes ÷ 4	Voltage in Volts	Inlet Gas Flow in Scale Units	Outlet Gas Flow	
					FT^3	Sec
85	40	22	680	46.2	Cathode	Failure
101	18	22	560	31.8	1.0	13.39
102	20	21	570	33.5	1.0	12.64
103	22	19.5	585	35.3	1.0	11.80
104	24	19.5	600	36.9	1.5	15.60
105	26	18.5	620	38.4	1.0	11.00

Test No.	Water Flow in LB/HR				Water Temperature Difference in °C			
	Radiation	Anode	Cathode	Anode Gas	Radiation	Anode	Cathode	Anode Gas
85	148	555	884	1494	3.28	8.53	15.12	28.2
101	151	525	904	1522	2.72	10.47	5.86	25.9
102	151	525	904	1519	2.72	9.74	5.61	27.3
103	151	525	904	1519	2.38	9.00	5.86	26.3
104	151	525	904	1519	2.26	8.15	6.58	25.6
105	151	525	904	1517	2.04	8.03	8.30	25.0

TABLE I. CONT.

Total Energy Balance, Raw Data

Test No.	Pressure in PSIG	Current in Amperes ÷4	Voltage in Volts	Inlet Gas Flow in Scale Units	Outlet Gas Flow	
					FT^3	Sec.
106	28	17.5	640	40.0	1.0	10.25
107	30	17	650	41.4	1.5	14.86
108	18	21	545	32.4	1.0	15.17
109	20	20	560	34.1	1.0	14.99
110	22	19	580	35.8	1.0	13.36
111	24	18.5	600	37.5	1.0	12.47

Test No.	Water Flow in LB/HR				Water Temperature Difference in °C			
	Radiation	Anode	Cathode	Anode Gas	Radiation	Anode	Cathode	Anode Gas
106	151	525	899	1517	1.81	7.55	10.72	23.9
107	151	525	899	1517	1.58	7.30	10.98	23.5
108	151	530	914	1532	2.26	10.22	10.42	23.2
109	151	530	914	1532	2.26	9.50	10.72	23.5
110	151	530	911	1532	2.04	8.53	12.43	23.2
111	151	530	911	1532	1.81	8.03	12.93	23.0

TABLE I. CONT.

TOTAL ENERGY BALANCE, RAW DATA

Test No.	Pressure in PSIG	Current in Amperes ÷ 4	Voltage in Volts	Inlet Gas Flow in Scale Units	Outlet Gas Flow	
					FT^3	Sec
112	26	18	610	38.9	1.0	11.52
113	28	17.5	625	40.3	1.5	16.48
114	30	16.5	640	41.5	1.5	15.51
115	20	35	475	33.5	1.0	11.65
116	25	33	530	37.5	1.0	11.95
117	30	29.5	575	41.1	1.5	11.69

Test No.	Water Flow in LB/HR				Water Temperature Difference in °C			
	Radiation	Anode	Cathode	Anode Gas	Radiation	Anode	Cathode	Anode Gas
112	151	530	911	1532	1.81	7.54	13.18	22.7
113	151	530	911	1532	1.58	7.30	13.53	22.5
114	151	530	911	1532	1.58	7.06	13.67	22.1
115	150	525	884	1532	6.34	15.32	12.2	33.9
116	150	525	879	1532	5.43	13.62	14.63	34.4
117	150	525	879	1532	4.75	12.18	17.31	36.1

TABLE I. CONT.
TOTAL ENERGY BALANCE, RAW DATA

Test No.	Pressure in PSIG	Current in Amperes ÷ 4	Voltage in Volts	Inlet Gas Flow in Scale Units	Outlet Gas Flow	
					FT³	Sec
118	35	27	615	43.9	1.5	12.62
119	40	25	650	46.9	1.5	11.21
120	40	26	650	47.3	1.5	11.25
121	35	29	620	44.2	1.5	13.95
122	30	32	575	41.1	Cathode	Failure
123	25	18	625	36.4	1.5	13.93

Test No.	Water Flow in LB/HR				Water Temperature Difference in °C			
	Radiation	Anode	Cathode	Anode Gas	Radiation	Anode	Cathode	Anode Gas
118	150	525	879	1532	4.3	10.83	17.31	37.0
119	150	525	879	1532	3.84	9.74	18.04	36.3
120	146	525	884	1542	4.30	10.47	16.82	38.9
121	146	525	884	1542	4.41	11.69	20.07	39.4
122	146	525	884	1542	4.97	13.40	22.7	38.9
123	150	500	814	1522	1.58	8.53	6.59	28.2

TABLE I. CONT.
TOTAL ENERGY BALANCE, RAW DATA

Test No.	Pressure in PSIG	Current in Amperes ÷ 4	Voltage in Volts	Inlet Gas Flow in Scale Units	Outlet Gas Flow	
					FT^3	Sec
124	25	21	610	36.5	1.5	14.97
125	25	26	580	37.3	1.0	10.58
126	25	29.5	558	36.9	1.0	10.52
127	25	32	550	37.0	1.0	10.80
128	20	35	495	32.8	1.0	12.64

Test No.	Water Flow in LB/HR				Water Temperature Difference in °C			
	Radiation	Anode	Cathode	Anode Gas	Radiation	Anode	Cathode	Anode Gas
124	150	500	814	1527	1.58	10.34	8.54	30.6
125	150	500	814	1522	3.51	12.19	9.03	32.7
126	150	500	816	1522	4.30	13.62	10.73	36.0
127	150	500	816	1522	4.64	15.34	12.69	39.0
128	150	505	819	1542	4.98	17.03	14.89	36.3

TABLE I. CONT.
TOTAL ENERGY BALANCE, RAW DATA

Test No.	Current in Amperes	Voltage in Volts	Power in Kilowatts	Losses in Kilowatts				
				Radiation	Anode	Cathode	Anode Gas	Cathode Gas
73	104	520	54.1	0.35	3.62	4.10	20.8	25.23
74	96	555	53.3	0.27	3.12	3.97	19.9	26.04
75	88	590	51.9	0.25	2.84	3.99	19.7	25.12
76	80	610	48.8	0.22	2.49	4.34	19.0	22.75
77	100	600	60.0	0.30	3.20	5.48	21.4	29.62
78	108	550	59.4	0.34	3.55	5.76	20.4	29.35

Test No.	Pressure in PSIG	Gas Flow in Grams/Min.			Gas Enthalpy in BTU/LB		
		Total	Anode	Cathode	Total	Anode	Cathode
73	18	19.3	8.85	10.5	61,900	61,100	62,500
74	20	21.9	9.20	12.7	55,200	56,300	53,400
75	22	24.0	9.88	14.1	48,600	51,900	47,100
76	24	26.2	10.10	16.1	41,700	49,000	35,700
77	24	25.9	9.65	16.3	51,200	57,600	46,800
78	20	22.7	8.10	14.6	56,900	65,400	52,200

TABLE II

TOTAL ENERGY BALANCE, RESULTS

Test No.	Current in Amperes	Voltage in Volts	Power in Kilowatts	Losses in Kilowatts				
				Radiation	Anode	Cathode	Anode Gas	Cathode Gas
79	108	650	57.1	0.25	2.63	5.70	20.0	28.52
80	88	680	54.4	0.22	2.20	5.76	18.9	27.32
81	80	515	63.8	0.36	4.25	8.96	21.4	28.83
82	124	572	64.0	0.35	3.84	8.84	22.6	28.37
83	112	620	64.5	0.33	3.20	8.05	23.5	29.42
84	104	650	62.4	0.30	2.85	7.37	23.1	28.78

Test No.	Pressure in PSIG	Gas Flow in Grams/Min.			Gas Enthalpy in BTU/LB		
		Total	Anode	Cathode	Total	Anode	Cathode
79	28	30.4	9.81	20.6	41,700	53,100	36,200
80	32	33.9	11.74	22.2	35,700	42,000	32,200
81	20	23.5	7.89	15.6	55,500	70,500	48,100
82	25	27.8	9.20	18.6	47,700	63,800	39,700
83	30	32.4	10.81	21.6	42,600	56,600	35,600
84	35	36.6	11.60	25.0	37,000	51,800	30,100

Table II Cont.
Total Energy Balance, Results

Test No.	Current in Amperes	Voltage in Volts	Power in Kilowatts	Losses in Kilowatts				
				Radiation	Anode	Cathode	Anode Gas	Cathode Gas
85	88	680	57.2	0.26	2.49	7.03	22.2	25.22
101	88	560	49.3	0.22	2.89	2.78	20.7	22.71
102	84	570	47.9	0.22	2.69	2.66	21.8	20.53
103	78	585	45.6	0.19	2.48	2.78	21.0	19.15
104	78	600	46.8	0.18	2.25	3.13	20.4	20.84
105	74	620	45.9	0.16	2.22	3.94	19.9	19.68

Test No.	Pressure in PSIG	Gas Flow in Grams/Min.			Gas Enthalpy in BTU/LB		
		Total	Anode	Cathode	Total	Anode	Cathode
85	40	40.8	—	—	29,200	—	—
101	18	20.7	10.23	10.5	54,500	52,700	56,200
102	20	22.7	10.82	11.9	48,500	52,400	44,900
103	22	24.6	11.60	13.0	42,500	47,100	38,500
104	24	26.6	13.18	13.4	40,500	40,500	41,500
105	26	28.5	12.44	16.0	36,300	41,700	32,200

TABLE II CONT.
TOTAL ENERGY BALANCE, RESULTS

Test No.	Current in Amperes	Voltage in Volts	Power in Kilowatts	Losses in Kilowatts				
				Radiation	Anode	Cathode	Anode Gas	Cathode Gas
106	70	640	44.8	0.14	2.08	5.08	19.1	18.40
107	68	650	44.2	0.13	2.02	5.19	18.7	18.16
108	84	545	45.8	0.18	2.85	4.93	18.7	19.14
109	80	560	44.8	0.18	2.65	5.15	18.9	17.92
110	76	580	44.1	0.16	2.42	5.96	18.7	16.86
111	74	600	44.4	0.14	2.24	6.20	18.6	17.22

Test No.	Pressure in PSIG	Gas Flow in Grams/Min.			Gas Enthalpy in BTU/LB		
		Total	Anode	Cathode	Total	Anode	Cathode
106	28	30.6	13.36	17.2	31,600	37,300	29,100
107	30	32.3	13.84	18.5	29,900	35,300	25,800
108	18	20.9	9.05	11.8	47,200	53,800	42,300
109	20	23.1	9.14	14.0	41,600	53,800	33,500
110	22	25.0	10.24	14.8	36,600	47,500	29,900
111	24	27.0	11.00	16.0	34,700	44,100	28,200

TABLE II CONT.

TOTAL ENERGY BALANCE, RESULTS

Test No.	Current in Amperes	Voltage in Volts	Power in Kilowatts	Losses in Kilowatts				
				Radiation	Anode	Cathode	Anode Gas	Cathode Gas
112	72	610	43.9	0.14	2.11	6.31	18.3	17.04
113	70	625	43.75	0.13	2.04	6.49	18.1	16.99
114	66	640	42.2	0.13	1.97	6.55	17.8	15.75
115	140	475	66.5	0.50	4.23	5.67	27.4	28.70
116	132	530	69.9	0.43	3.76	6.77	27.7	31.24
117	118	575	67.8	0.38	3.37	8.00	29.1	26.95

Test No.	Pressure in PSIG	Gas Flow in Grams/Min.			Gas Enthalpy in BTU/LB		
		Total	Anode	Cathode	Total	Anode	Cathode
112	26	29.0	11.88	17.1	31,900	40,300	26,300
113	28	30.9	12.47	18.4	29,800	37,900	25,300
114	30	32.6	13.22	19.4	26,200	35,200	21,400
115	20	22.7	11.84	10.9	64,100	60,100	68,300
116	25	27.4	12.50	14.9	55,900	57,500	54,900
117	30	32.3	13.98	18.3	44,700	54,100	38,500

Table II Cont.
Total Energy Balance, Results

Test No.	Current in Amperes	Voltage in Volts	Power in Kilowatts	Losses in Kilowatts				
				Radiation	Anode	Cathode	Anode Gas	Cathode Gas
118	108	615	66.4	0.34	2.99	8.00	29.9	25.17
119	100	650	65.0	0.30	2.69	8.35	29.3	24.36
120	104	650	67.6	0.33	2.89	7.83	31.6	24.95
121	116	620	71.9	0.34	3.23	9.64	32.0	26.69
122	128	575	73.5	0.37	3.70	9.49	31.6	28.34
123	72	625	45.0	0.12	2.24	2.82	22.6	17.22

Test No.	Pressure in PSIG	Gas Flow in Grams/Min.			Gas Enthalpy in BTU/LB		
		Total	Anode	Cathode	Total	Anode	Cathode
118	35	36.7	16.26	20.4	39,200	47,900	32,300
119	40	41.4	16.96	24.4	33,900	45,000	26,200
120	40	41.8	16.42	25.4	35,300	50,000	25,800
121	35	36.9	14.71	22.2	41,500	56,500	31,500
122	30	32.3	—	—	48,300	—	—
123	25	26.5	14.73	11.8	39,300	40,000	38,100

TABLE II CONT.
TOTAL ENERGY BALANCE, RESULTS

Test No.	Current in Amperes	Voltage in Volts	Power in Kilowatts	Losses in Kilowatts				
				Radiation	Anode	Cathode	Anode Gas	Cathode Gas
124	84	610	51.2	0.12	2.72	3.65	24.5	20.21
125	104	580	60.4	0.28	3.21	3.86	26.2	26.85
126	118	558	65.8	0.34	3.59	4.60	28.9	28.37
127	128	550	70.4	0.37	4.04	5.43	31.3	29.26
128	140	495	69.3	0.39	4.53	6.39	29.4	28.59

Test No.	Pressure in PSIG	Gas Flow in Grams/Min.			Gas Enthalpy in BTU/LB		
		Total	Anode	Cathode	Total	Anode	Cathode
124	25	26.6	13.72	12.9	43,800	46,500	40,900
125	25	27.3	12.92	14.4	50,500	52,700	48,600
126	25	27.0	13.00	14.0	55,100	57,800	52,700
127	25	27.1	12.69	14.4	58,000	64,100	52,900
128	20	22.2	10.72	11.5	67,800	71,200	64,600

Table II Cont.
Total Energy Balance, Results

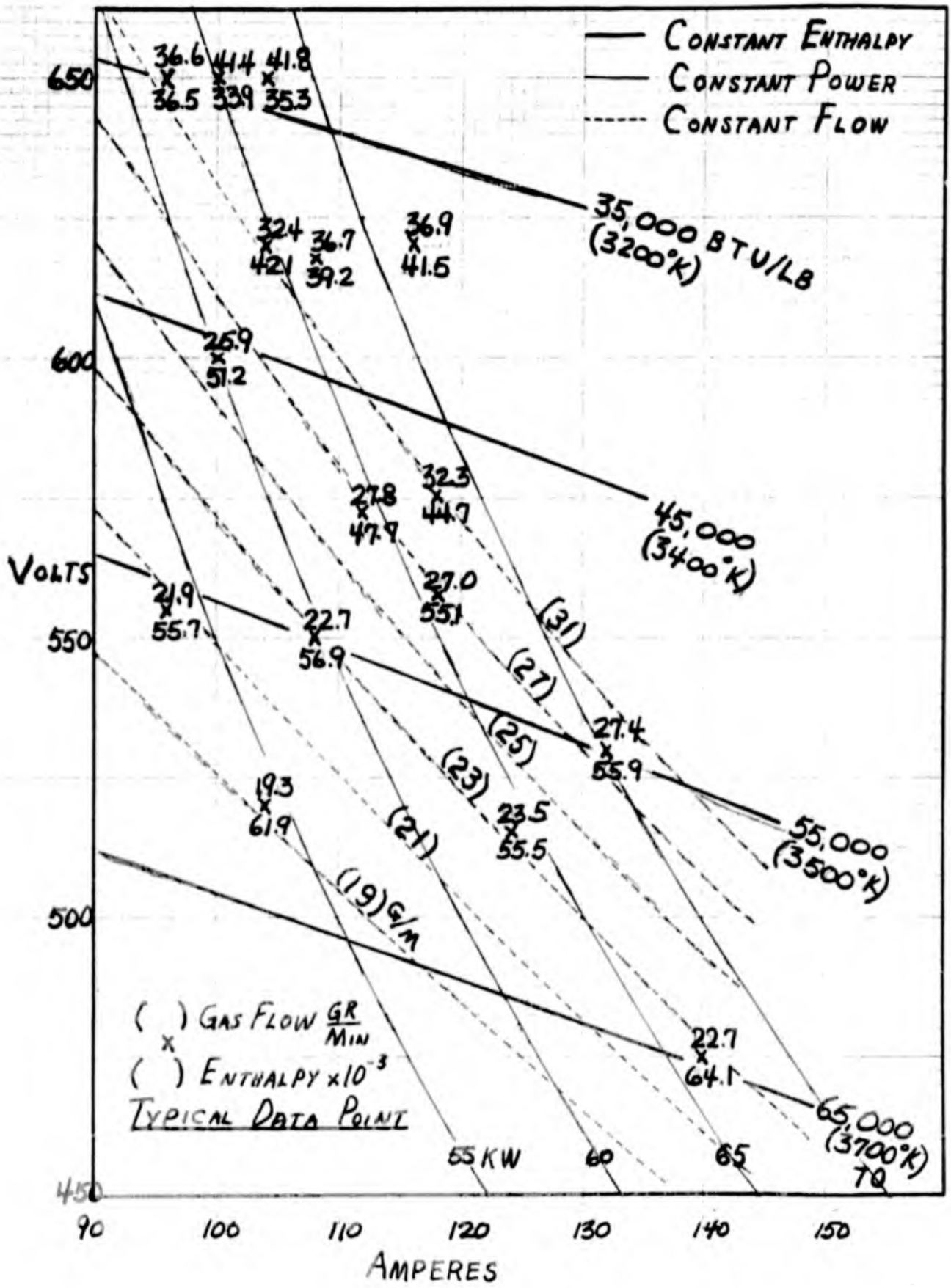

Figure 8

Arc Operating Conditions

V. Results and Interpretation

The results of this experiment fall into three categories: characteristic curves, total energy balance, and electrode losses. Electrode losses are really a part of the total energy balance result but because of the immediate application of this information, it is treated separately. The results will be discussed in the order stated and each discussion will be supplemented by several graphs. An estimate of error limits concludes the chapter.

Characteristic Curves

Stable Region. Figure 8 is a graphical description of arc operation above ninety amperes. The dotted lines are the constant mass flow characteristic curves. The light solid lines are constant power curves and the heavy solid lines are constant enthalpy curves. The experiment was not exhaustive enough to produce an operating envelope.

The characteristic curves in this region exhibit the negative nature expected of the arc column alone although this figure includes the voltage of the fall regions. The constant current intercepts of the flow rate curves illustrate the expected increase in voltage and power and decrease in enthalpy for an increase of flow rate.

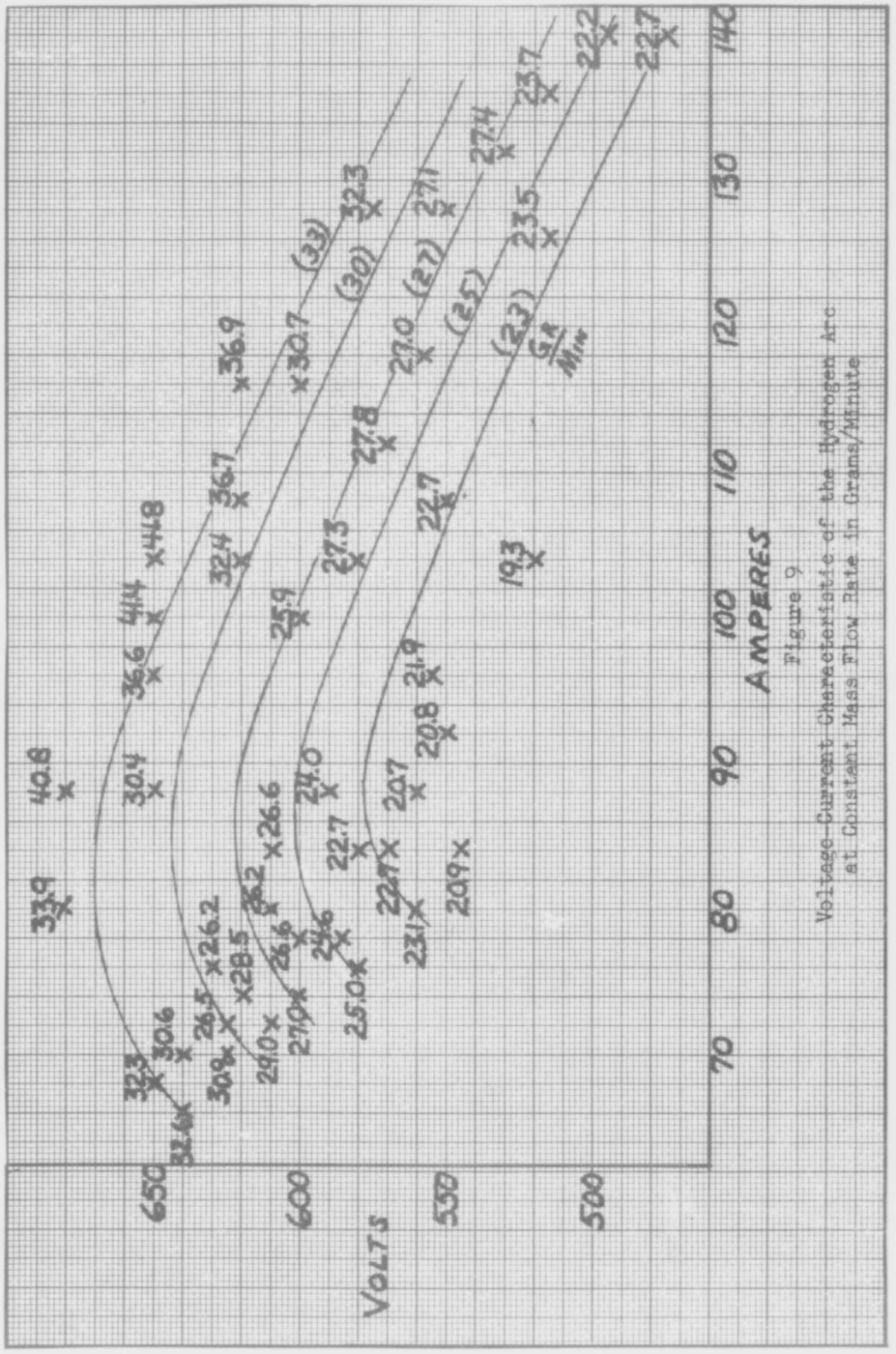

Figure 9

Voltage-Current Characteristic of the Hydrogen Arc at Constant Mass Flow Rate in Grams/Minute

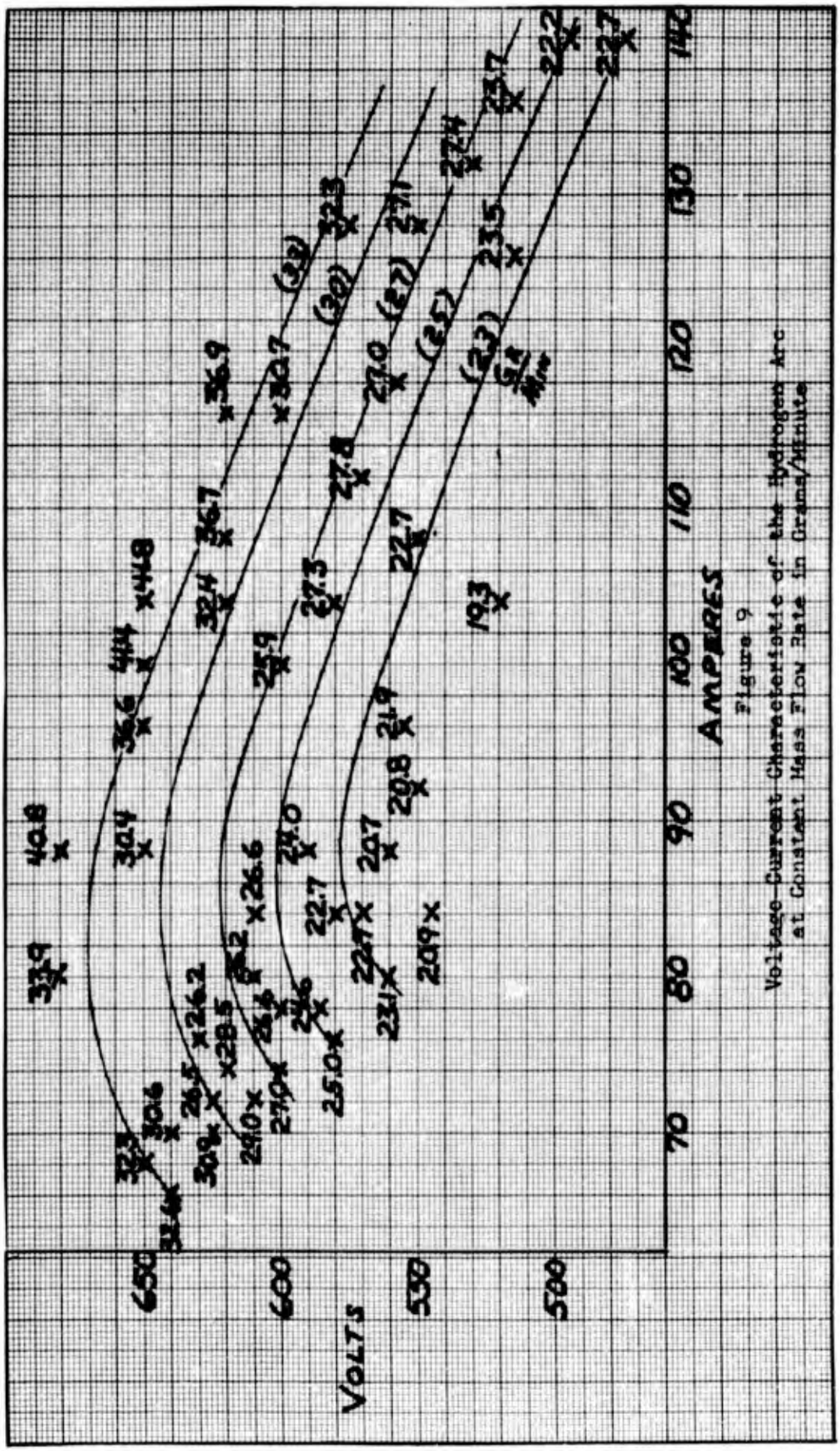
VOLTS
650
600
550
500
AMPERES
70
80
90
100
110
120
130
140
Voltage-Current Characteristic of the Hydrogen Arc
at Constant Mass Flow Rate in Grams/Minute

Figure 9

Unstable Region. The constant flow rate characteristic curves for the total range of current covered are shown in Figure 9. The positive slope at low current is unexpected. The fact that the curves are uniform and orderly is also unusual since the cathode fall is included in the voltage. As mentioned earlier the arc at the cathode is very unstable and erratic and this would normally lead to non-uniformity. Similar curves do not exist for nitrogen because of the expected disorderly arrangement.

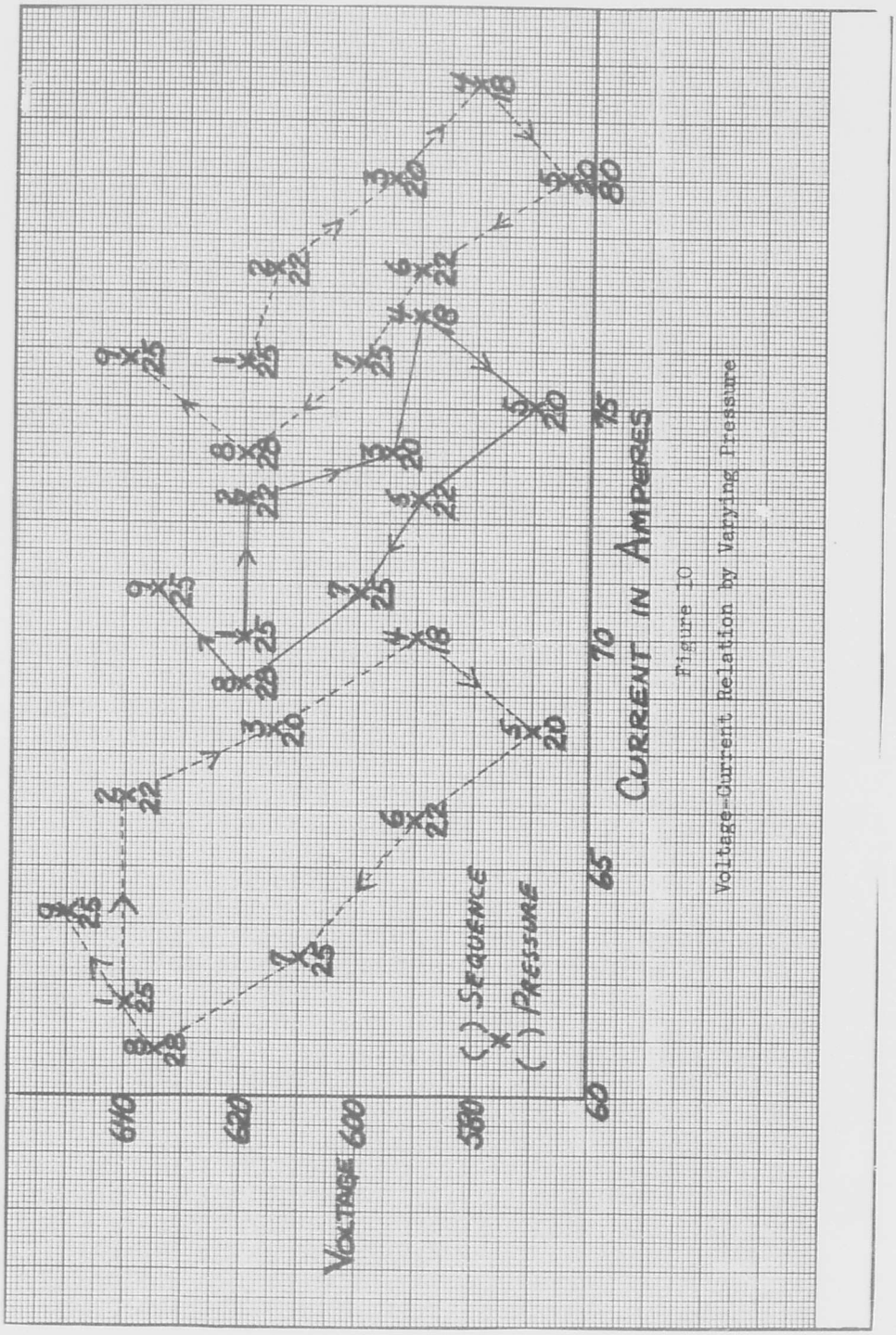

Figure 10

Voltage-Current Relation by Varying Pressure

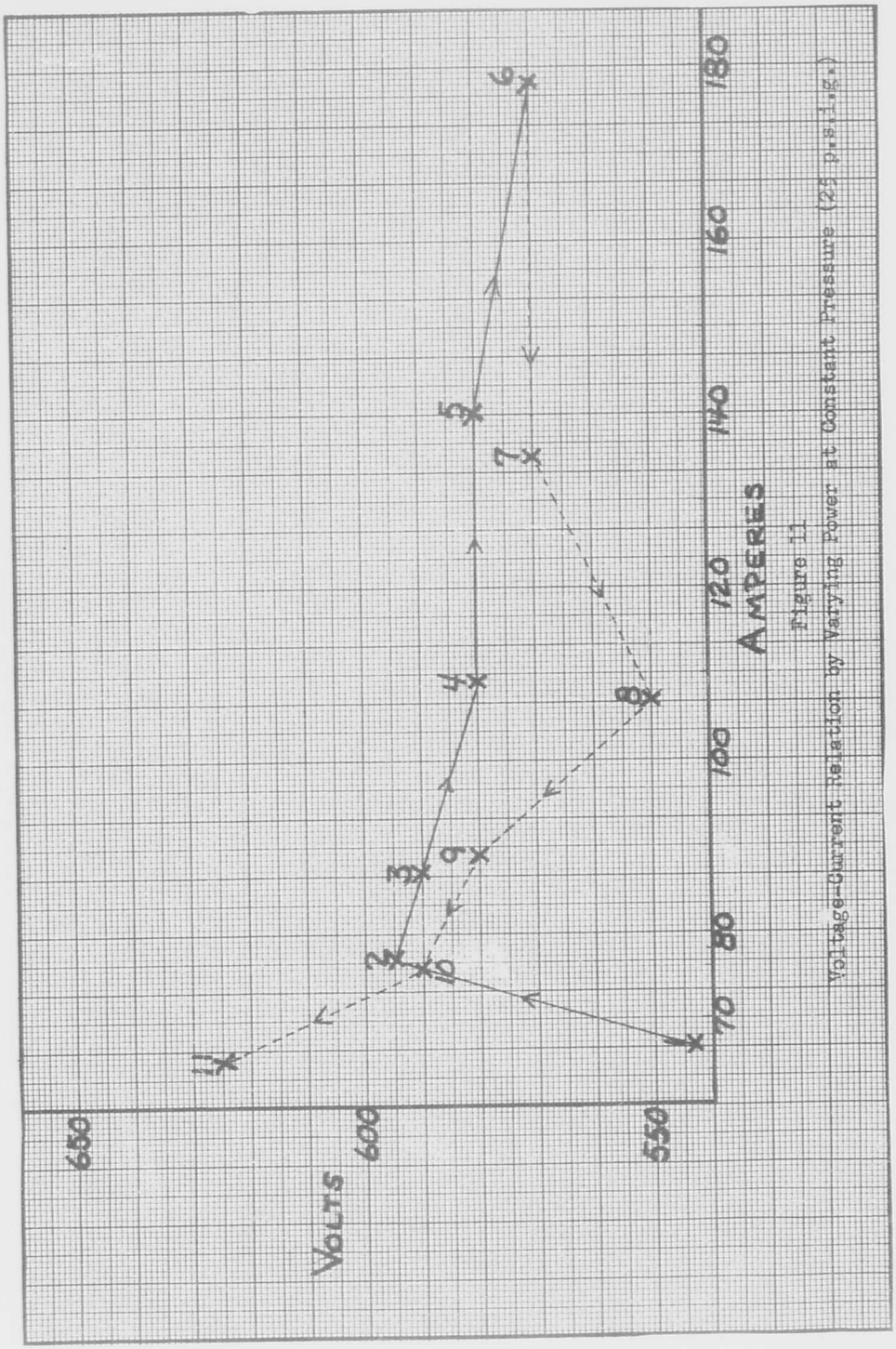

Figure 11

Voltage-Current relation by Varying Power at Constant Pressure (25 p.s.i.g.)

The positive characteristic prompted further investigation. All data for hydrogen tests had been taken by varying the supply pressure upwards with a constant rectifier setting. A new series of tests was made at three different rectifier settings. From twenty-five p.s.i.g. the supply pressure was first decreased by increments to eighteen p.s.i.g., then increased to twenty-eight p.s.i.g., and finally returned to twenty-five p.s.i.g. Results of these tests are given in Figure 10.

A second series of tests was made at a constant supply pressure of twenty-five p.s.i.g. The power supply was varied in increments of current from sixty-six and one-half amps up to one hundred and seventy-eight amps and back down to sixty-five amps. As is shown by Figure 11, the positive characteristic is lost when the current is decreased. It may be presumed that this positive slope is not a stable condition since it can only be achieved upon starting.

Interpretation of this positive characteristic will not be undertaken. Two possible explanations have been advanced. Captain Richard Wingerson, Assistant Professor, Air Force Institute of Technology, Dayton, Ohio, suggested that it could be a matter of surface preparation at the cathode side. Doctor Emil Pfender, Scientist, Aeronautical Research Laboratory, Dayton, Ohio, thought that the presence of a preionized path could be a factor. Basic to both of these suggestions is the assumption that the higher voltage is due to a longer arc; the increase in arc length resulting from the cathode spot running around at a greater radius.

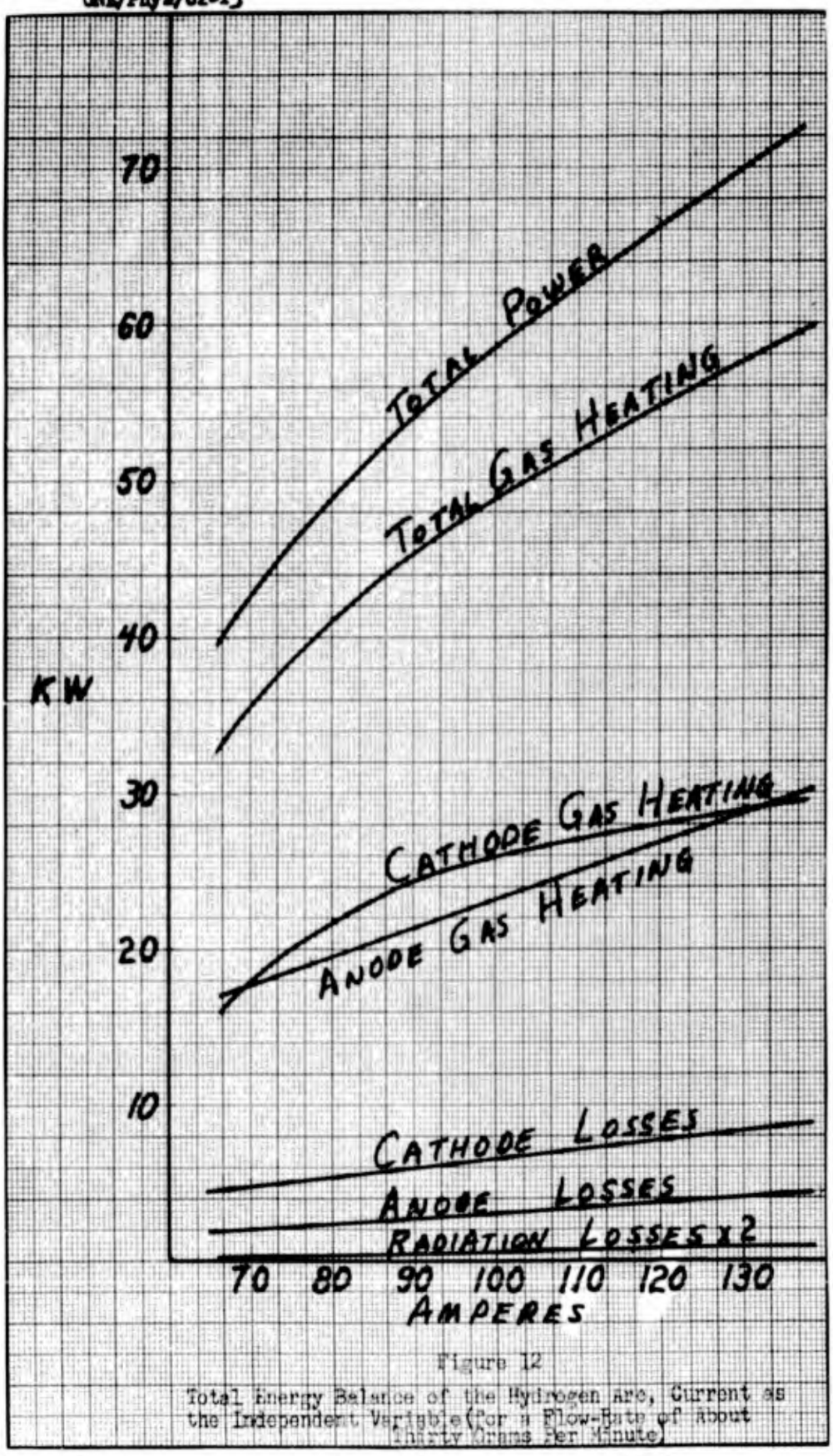

Figure 12

Total Energy Balance of the Hydrogen Arc, Current as the Independent Variable (For a Flow-Rate of About Thirty Grams Per Minute)

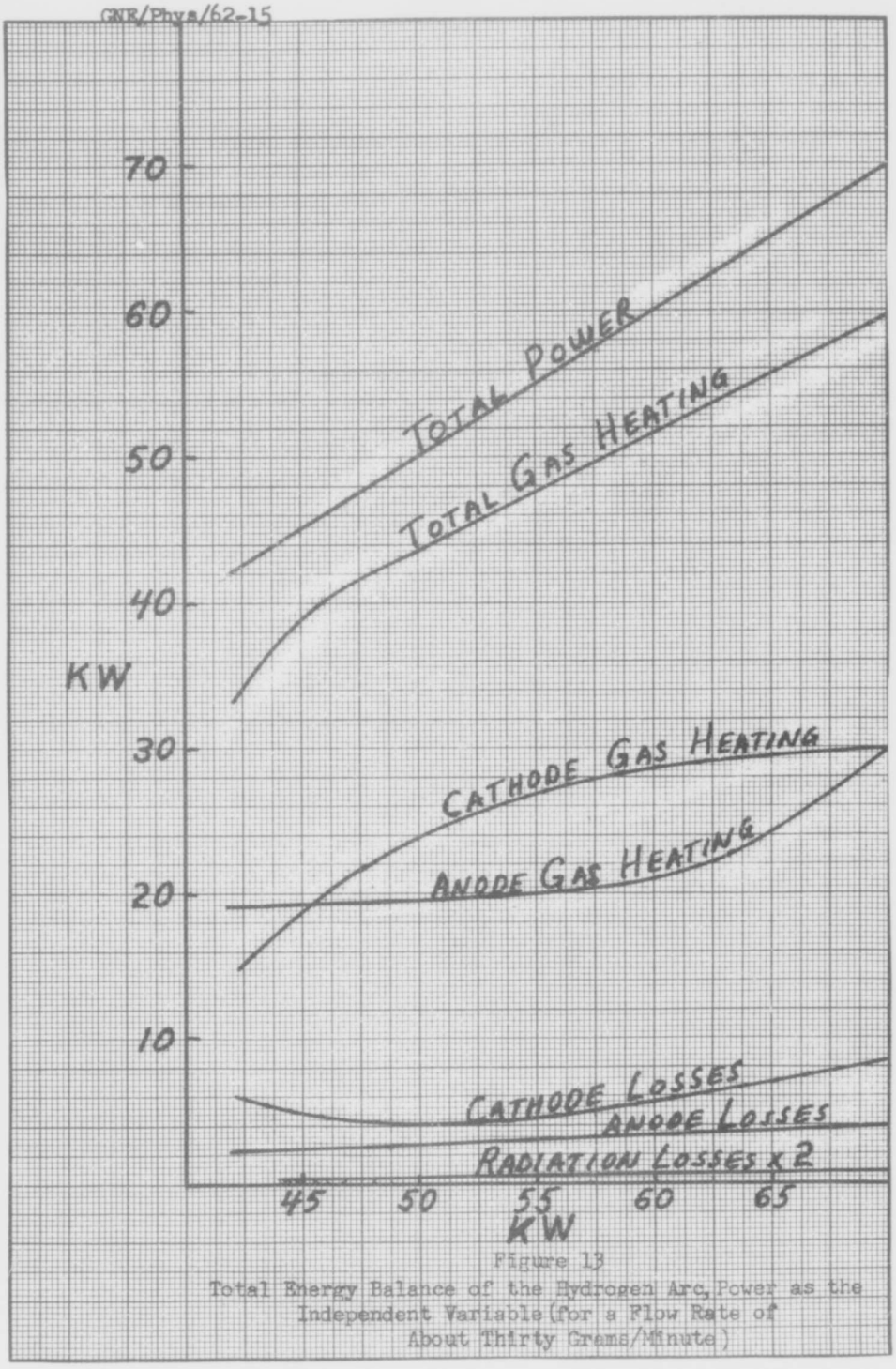

Figure 13
Total Energy Balance of the Hydrogen Arc, Power as the Independent Variable (for a Flow Rate of About Thirty Grams/Minute)

Total Energy Balance

General. The total energy balance over a range of current from sixty-six to one hundred and forty amperes is given in Figure 12. Curves are representative for a flow rate of approximately thirty grams per minute. Accurate, detailed graphs for each curve are given in subsequent figures. The cathode gas heating curve begins to straighten above ninety amperes which is also the point of change from positive to negative characteristic. The tendency for cathode gas heating to fall below anode gas heating at high currents is a consequence of the greater rate of increase of cathode losses compared to anode losses. Cathode losses will be covered on page 42. Figure 13 presents the total energy balance as a function of power input. This figure is for information and comparison only since current is the more sensitive parameter.

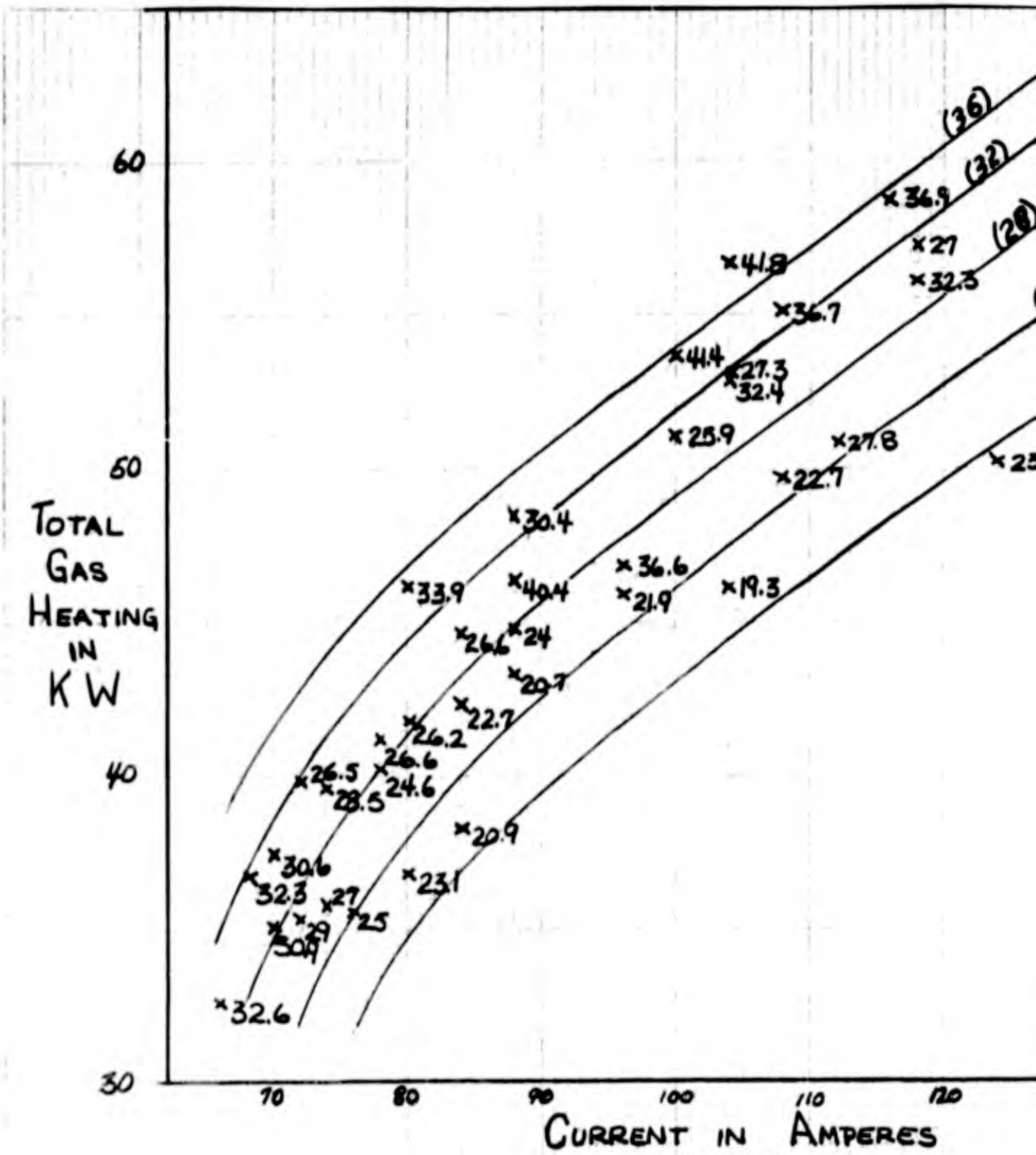

Figure 14

Total Gas Heating in the Hydrogen Arc

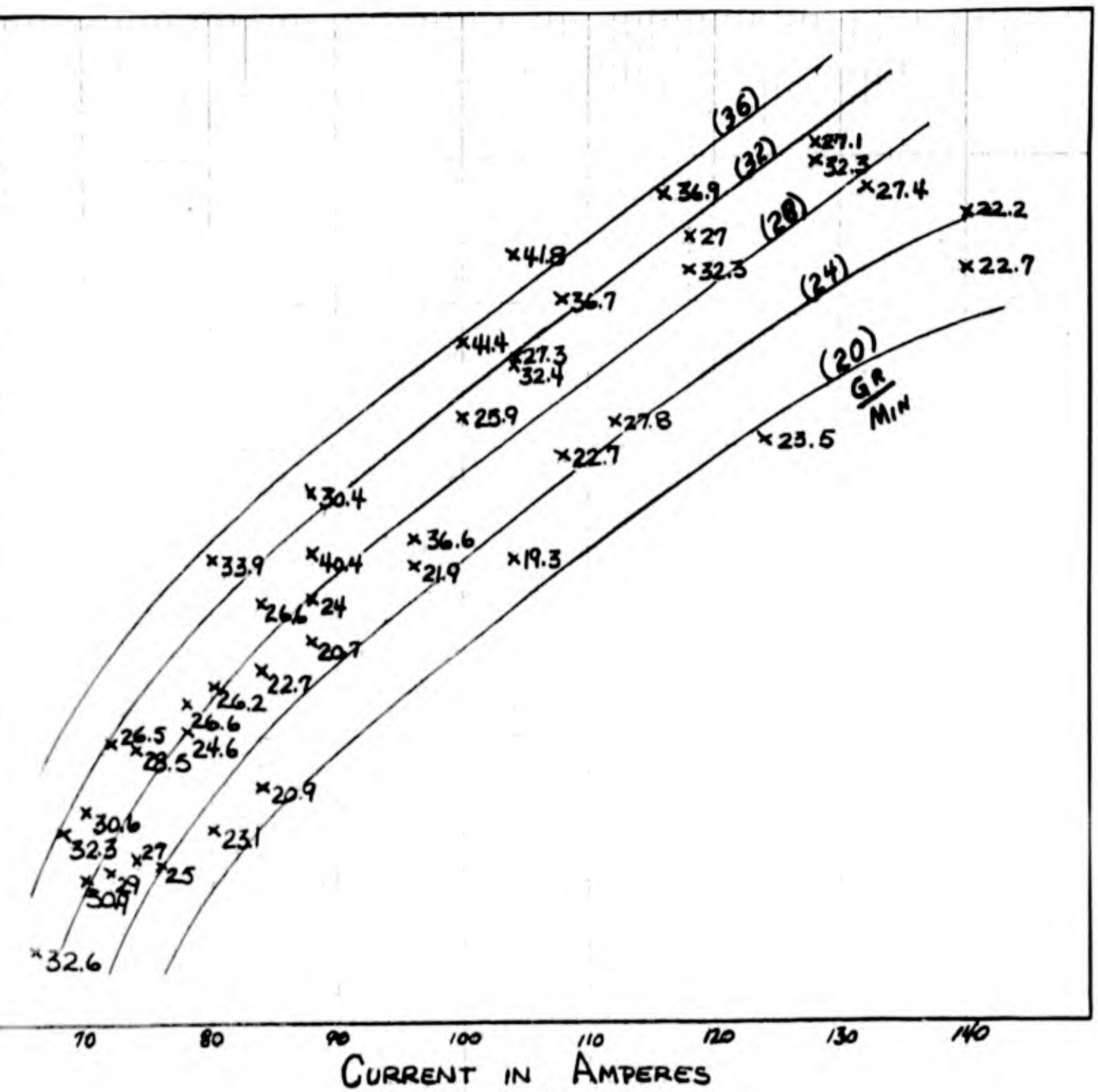

Figure 14

Total Gas Heating in the Hydrogen Arc

2

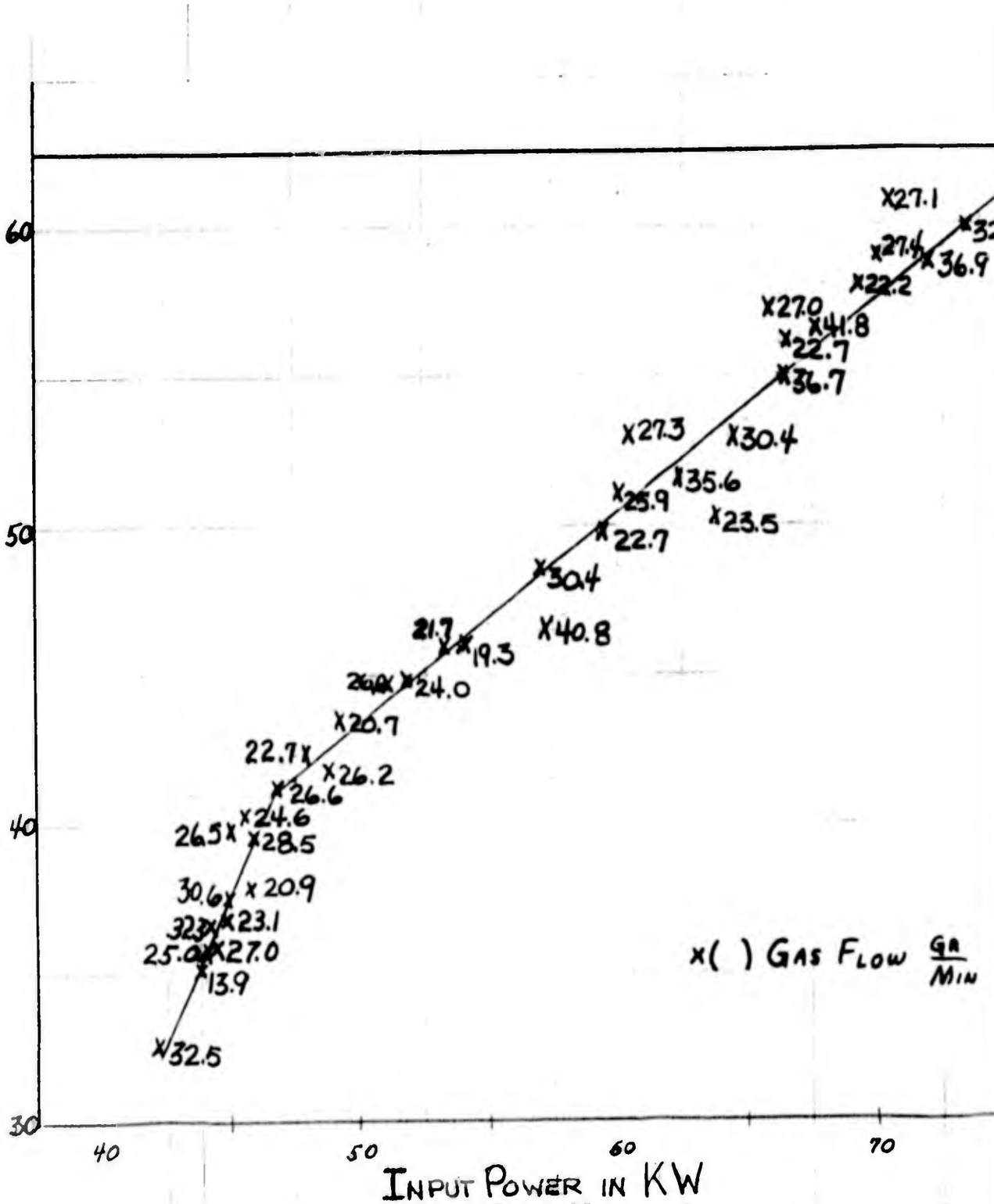

Figure 15
Gas Heating vs. Input Power

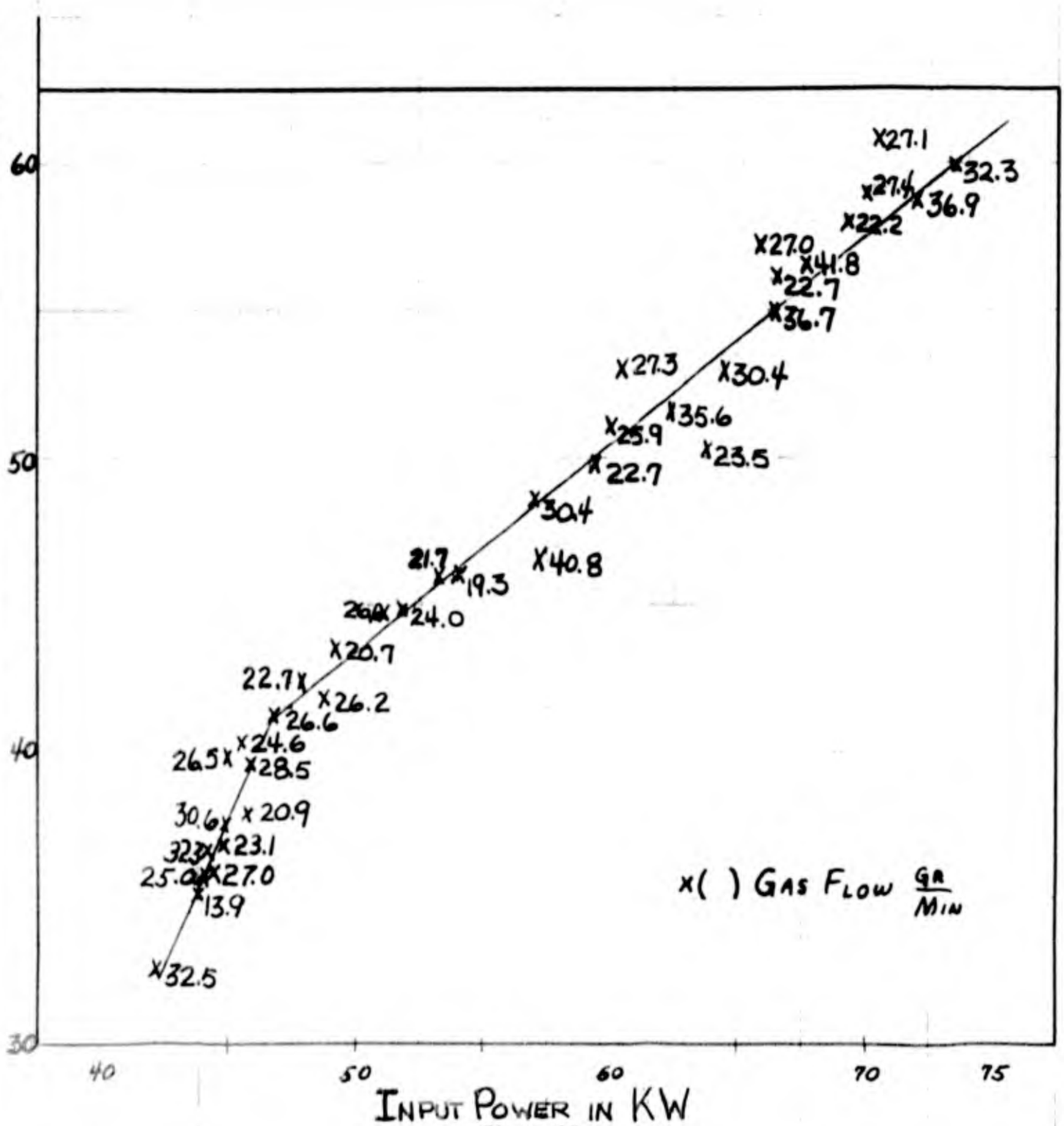

Figure 15
Gas Heating vs. Input Power

Total Gas Heating. Figure 14 shows the increase in gas heating at constant current due to increasing the flow rate or pressure. Enthalpy is decreased by increasing the flow rate but the arc diameter is decreased. At constant current a smaller arc diameter means an increase in axis temperature and this is the great advantage of whirl-stabilization.

Total gas heating as a function of input power is shown in Figure 15. Efficiency is about eighty-five percent. The break in the curve again corresponds to the change from positive to negative characteristic. There is no dependence of gas heating on flow rate when input power is the independent variable; therefore, an analysis of this efficiency curve is not possible.

Figure 16

Anode Gas Recycling, Gas Flow as Parameter

Figure 17
Cathode Gas Heating

Anode and Cathode Gas Heating. Anode gas heating is shown in Figure 16. Behavior with increasing flow rate is the same as for total gas heating. The contrast between anode and cathode gas heating, Figure 17, is remarkable. Because of the instability of the cathode spot and therefore the arc itself at the cathode side, sporadic heating is evident. Fortunately, this instability has no effect on the arc between the electrodes. (Ref. 7; 897).

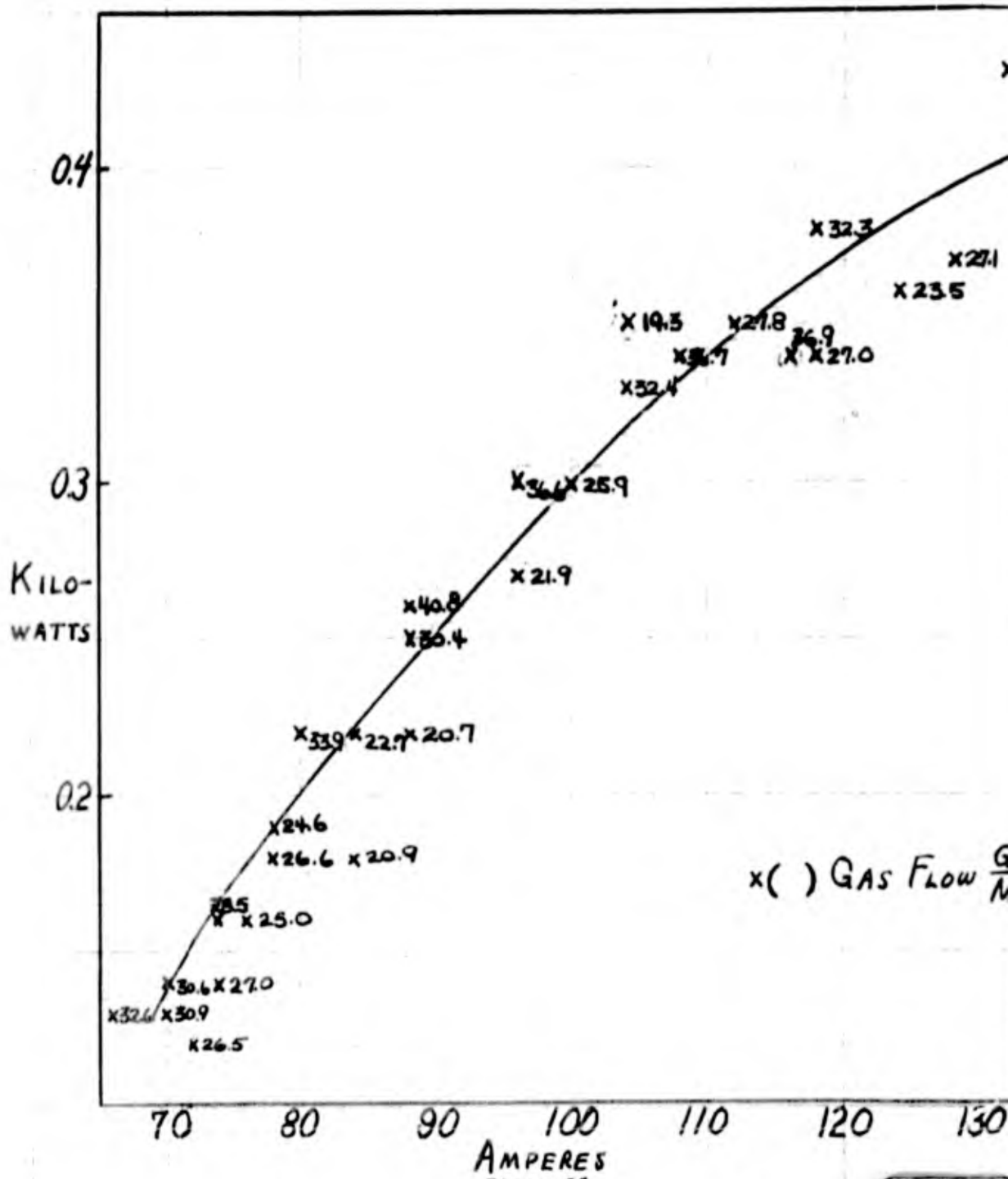

Figure 18

Radiated Power from the Hydrogen Arc (Radial Direction)

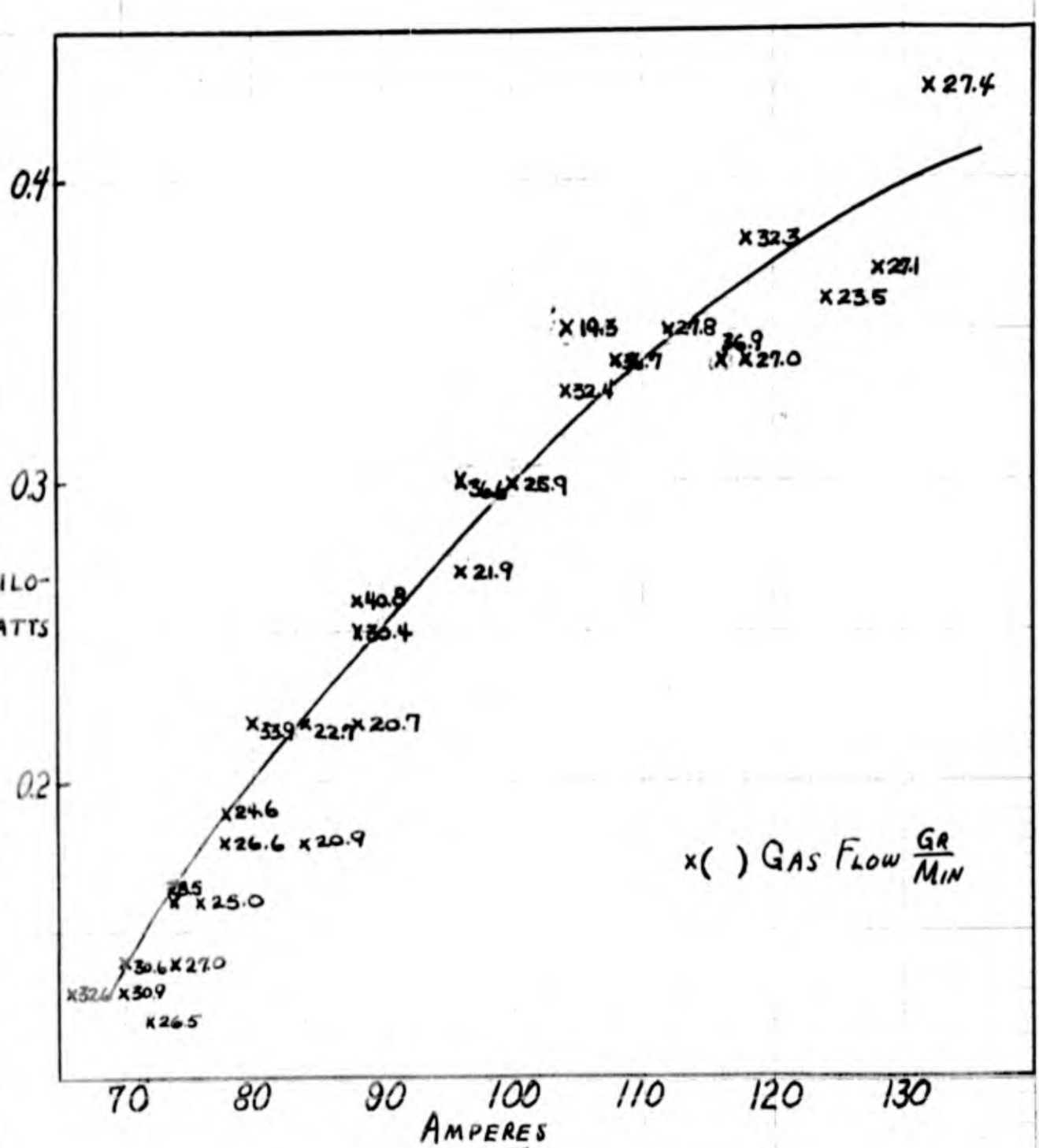

Figure 18

Radiated Power from the Hydrogen Arc (Radial Direction)

Radial Radiation Loss. Radial radiation as a function of current is shown in Figure 18. This measurement had the lowest degree of accuracy of all that were made because of the small temperature difference in the heated water. Error limits are about ten percent at one-hundred amperes. At constant current the radiation increases with increasing flow rate. This is attributed to the higher axis temperatures which result with higher flow rates and is an indication that the number of positive ions decreases with flow rate. The date for nitrogen shows a similar dependence on flow rate. The curve for nitrogen is steeper and straighter in the same range of current and the total amount of radiation is two to four times that of hydrogen at eighty and one hundred and forty amperes respectively.

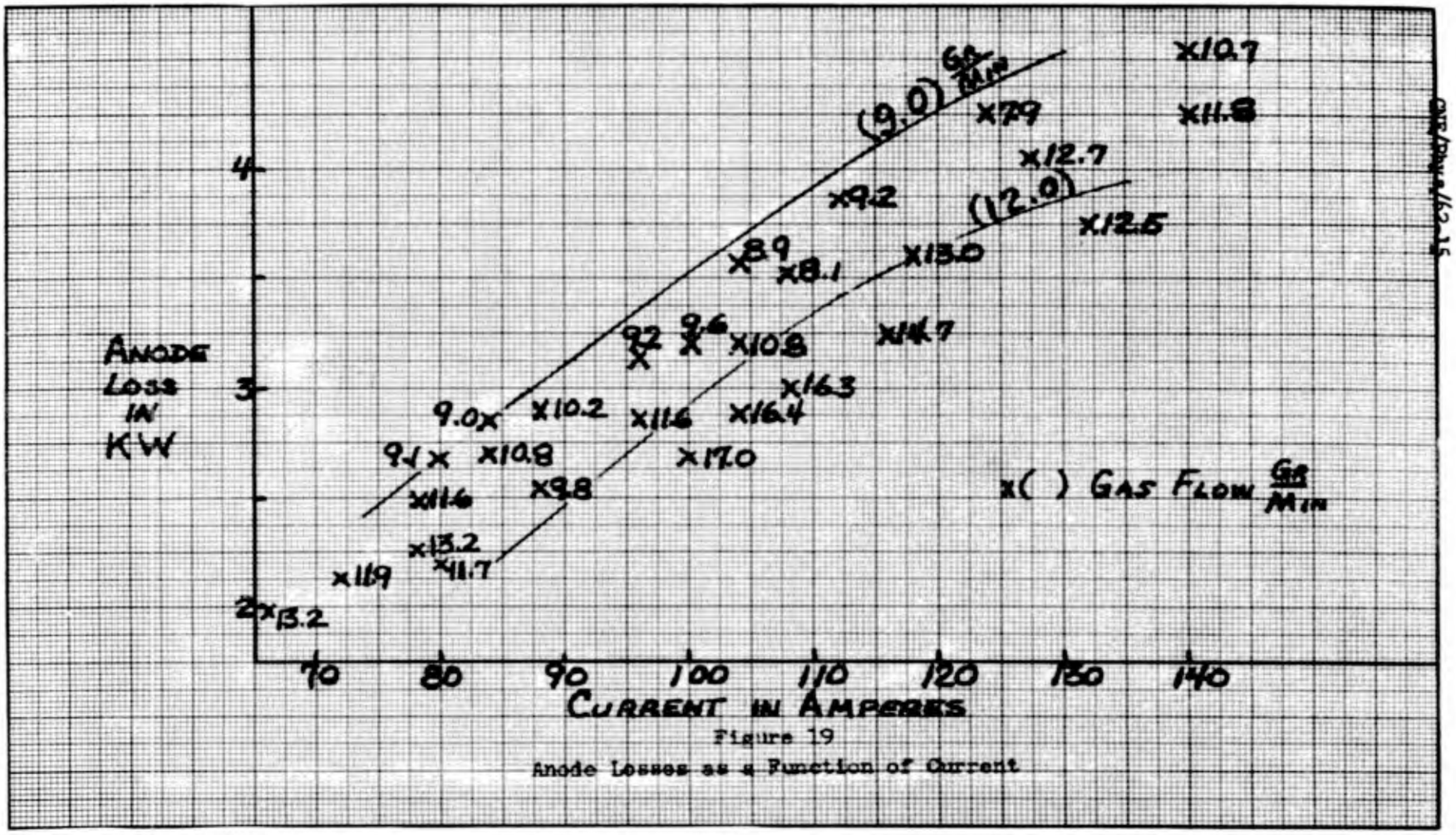

Figure 19

Anode Losses as a Function of Current

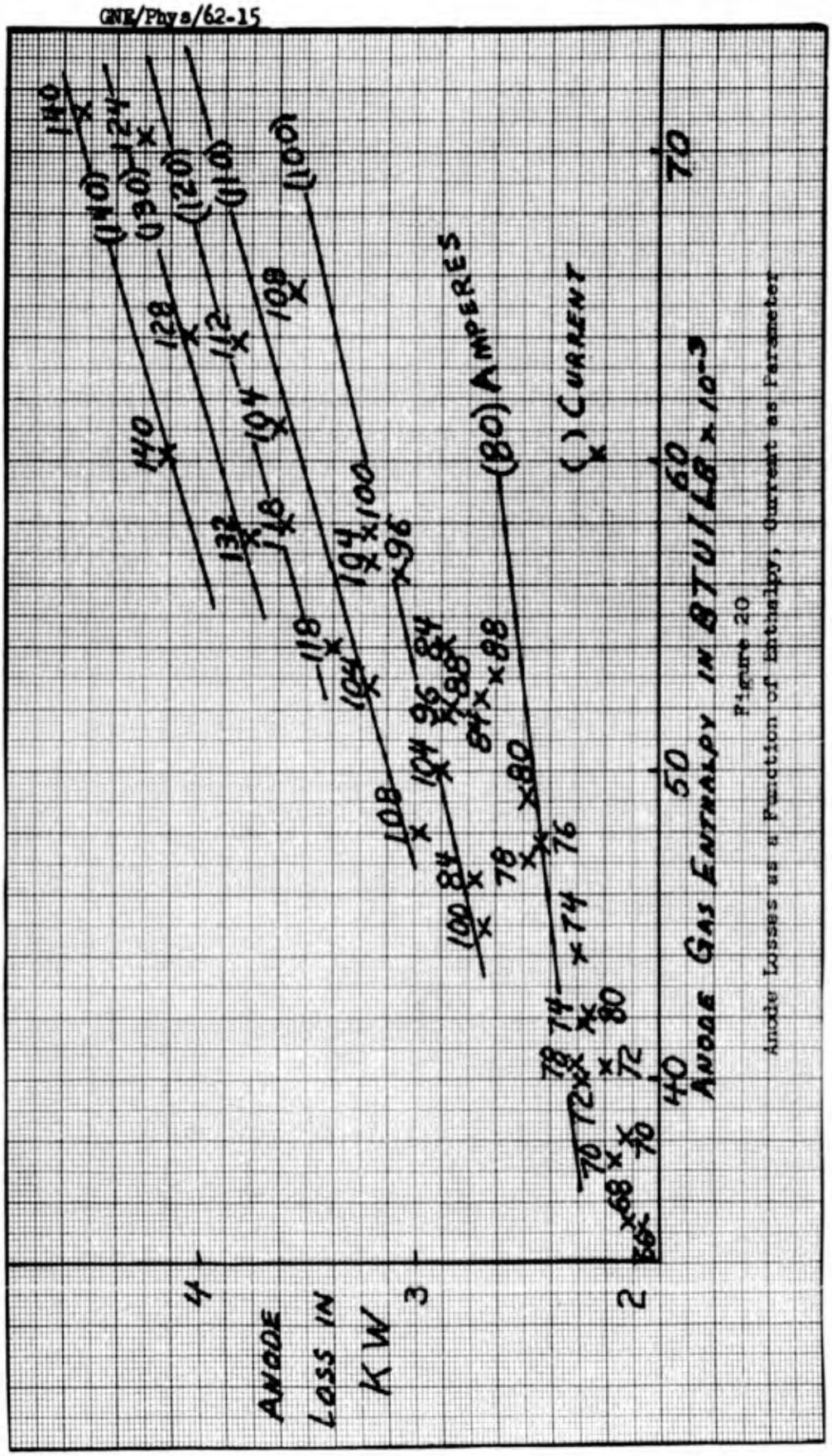

Figure 20

Anode Losses as a Function of Enthalpy, Current as Parameter

Electrode Losses

Anode Losses. Figures 19 and 20 present anode losses as a function of current and enthalpy, respectively. The increase in anode loss with decreasing flow rate shown in Figure 19 is attributed to increasing enthalpy. This dependence of anode loss on enthalpy is apparent from Figure 20. The main reason for Figure 19 is later comparison with a similar presentation of cathode losses.

The energy balance at the anode, neglecting radiation and vaporization, is:

$$Q = q_1 + q_2 + q_3 \qquad (14)$$

where

$q_1 = V_a I$ - (kinetic energy)

$q_2 = F_a I$ - (work function energy)

$q_3 = h(i_g - i_w)$ (heat transfer by convection)

From Figure 20 at a constant enthalpy of 60,000 BTU/lb and between the 100 ampere and 140 ampere constant current lines the following values can be obtained:

$Q = 900$ watts

$I = 40$ amperes

$q_3 = 0$

Then from equation (14)

$$900 = V_a (40) + F_a (40) \qquad (15)$$

and $F_a = 4.5$ ev (Ref. 5; 2558)

Solving equation (15)

$$V_a = 18 \text{ volts}$$

which is a reasonable value for the anode fall.

Also, from Figure 20 at 60,000 BTU/lb and 100 amperes

$$Q = 3225 \text{ watts}$$

Then from equation (4)

$$3225 = 100 (18 + 4.5) + q_3 \qquad (16)$$

and solving equation (16)

$$q_3 = 975 \text{ watts}$$

This value is useful for estimating the contribution of convective heating at the cathode side in the next section.

The slight convergence of the curves of Figure 20 at lower enthalpy and current may be a result of the unstable positive characteristic discussed earlier. The general parallelism of the curves indicates that the anode fall does not vary much with changing enthalpy or by association with changing flow rate.

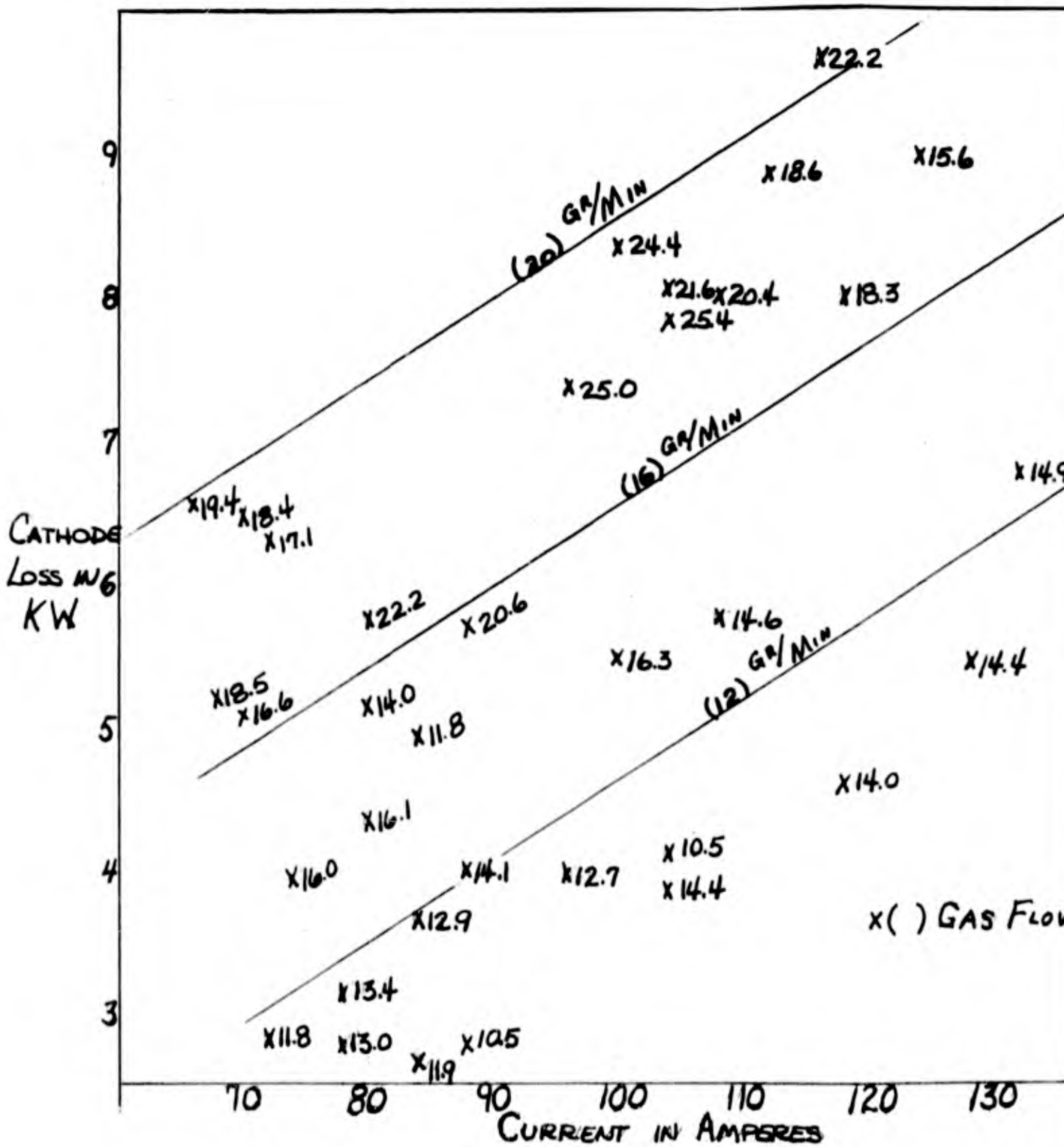

Figure 21
Cathode Losses as a Function of Current, Flow Rate as Parameter

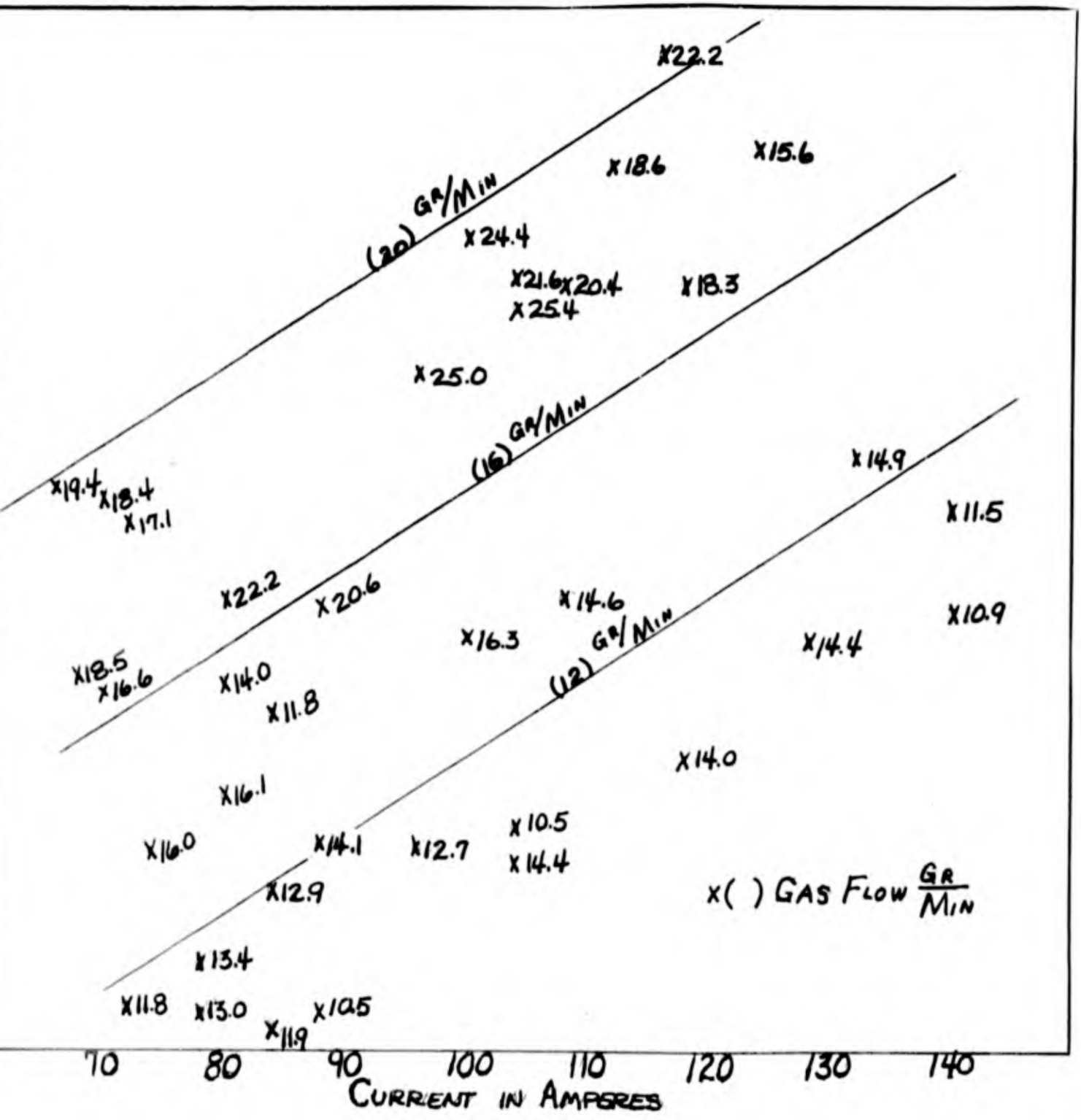

Figure 21
Cathode Losses as a Function of Current, Flow Rate as Parameter

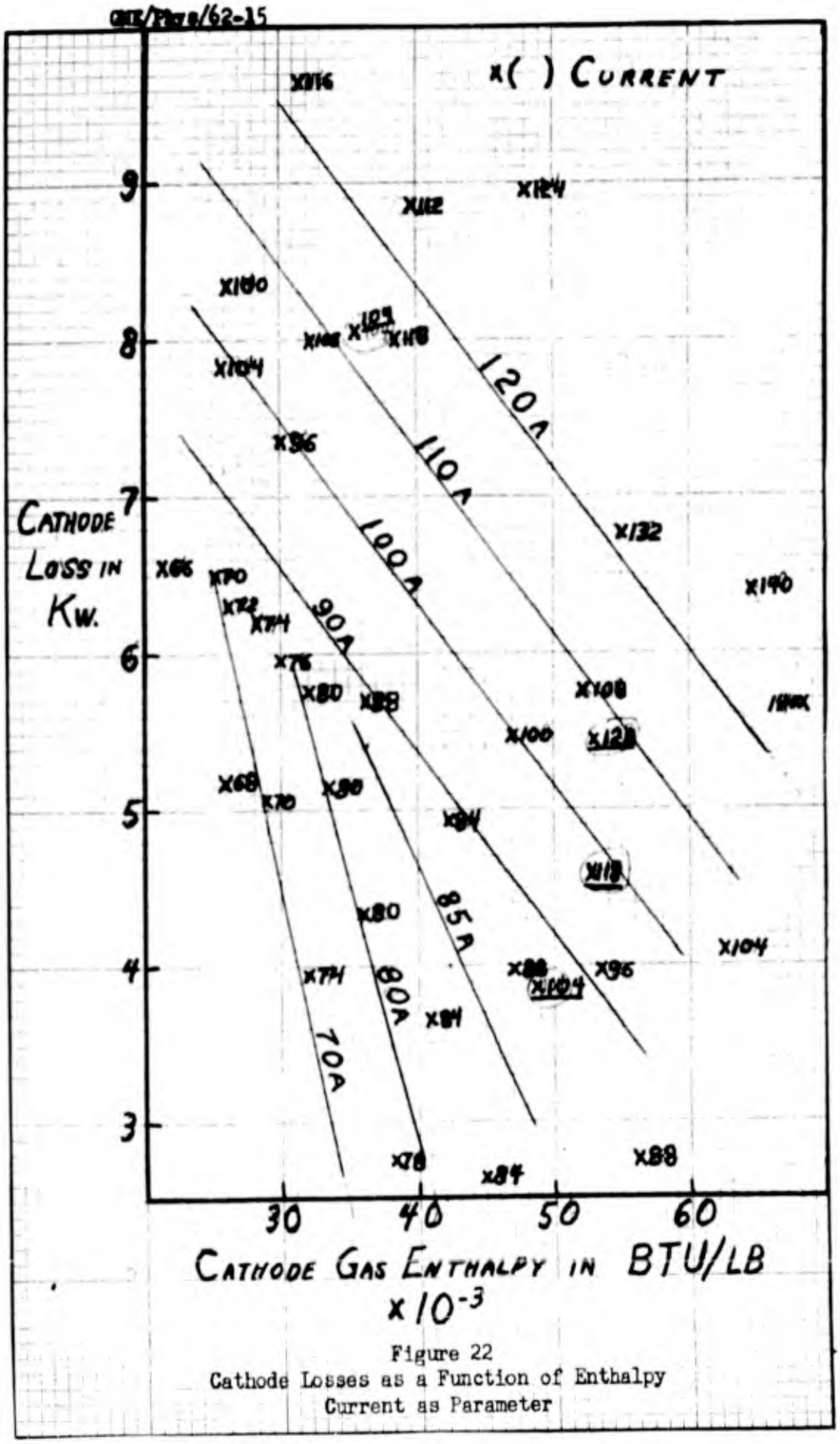

Figure 22
Cathode Losses as a Function of Enthalpy
Current as Parameter

Figures 21 and 22 present cathode losses as a function of current and enthalpy, respectively. Comparison of Figures 19 and 21 shows that anode and cathode losses are oppositely related to flow rate. For decreasing flow rates, anode losses increase while cathode losses decrease. Obviously then, some optimum condition should be achieved by restricting the flow rate at the cathode side.

Preliminary tests have been made with a cathode discharge hole diameter of one-eighth inch instead of three-sixteenths inch. The cathode lifetime was more than doubled and roughly fifty percent higher power levels were achieved without rapid deterioration. Another test with an anode hole diameter of one-quarter inch and a cathode hole diameter of one-eighth inch caused geometric instability of the arc channel.

The energy balance at the cathode neglecting radiation and vaporization is:

$$\dot{q} = q_1 + q_2 + q_3 - q_4 \qquad (17)$$

where

$q_1 = V_c I_+ a_k$ (kinetic energy)

$q_2 = I_+ (V_i - F_a)\, a_n$ (neutralization energy)

$q_3 = h\,(i_g - i_w)$ (heat transfer by convection)

$q_4 = I_- F_a a_e$ (work function energy)

a_k and a_n are accommodation coefficients resulting from reflection of positive ions and a_e is a correction which adjusts for thermionic or field emission.

In addition to the increase in the amount of heating mechanisms, the problem is further complicated by the instability at the cathode side. Therefore, quantitative analysis is not possible.

Figure 22 indicates a considerably higher V_c than did Figure 20 for the anode. Since V_c increases with increasing flow rate, q_1 will increase also. Apparently this effect is much stronger at the cathode side and overcomes any effects due to decreased enthalpy. According to the previous calculation heating by convection amounted to about thirty percent of anode losses. Assuming the same temperature profile at the cathode, this loss amounts to ten to twenty-five percent of cathode losses.

A decreasing V_c should cause the curves of Figure 4 to converge at high enthalpy (low flow rate). The data is not precise enough to reflect this tendency. If the tendency is actually not present, then the cathode fall is not influenced by the flow rate and some other explanation for high cathode losses at high flow rates must be made.

One possibility might be the supply of positive ions. It is conceivable that at lower flow rates the number of positive ions is not sufficient to carry the current thus requiring cathode emission of electrons. The resultant cooling would be two-fold. First, q_1 would be reduced linearly according to the lack of positive ions. Second, q_4, a cooling effect would be increased.

The results of the tests on nitrogen gas are insufficient for a similar analysis of anode and cathode losses. From the small amount of questionable data available, there did not seem to be any trends similar to those noted with hydrogen. If such is the case, it is readily explainable. Nitrogen bulk temperatures (from T-S diagrams) were more than double those for hydrogen at the same power level. This indicates a much steeper temperature profile for hydrogen as is expected from its greater thermal conductivity. Consequently the gas near the wall will have a higher temperature in the case of nitrogen and the heat transfer by convection will be increased thus masking other effects. Also no band of relatively cool gas exists to increase the anode and cathode fall. Finally, the degree of ionization is much higher at the temperatures experienced with nitrogen so that the supply of positive ions would not be critical.

Instrument	Instrument Limit of Error	Estimated Reading Error
Millivoltmeter	0.5 mv	0.5 mv
Voltmeter	10 v	5 v
Water-Flow Meter	10 lb/hr	5 lb/hr
Gas-Flow Meter	1 unit (1.5%)	0.5 units (0.75%)

Table III

Error Limits

Limit of Error

The instrument limit of error and the estimated error in reading the instrument are given in Table III. The limit of error for each of the principal values in the experiment can be estimated using the information from Table II and Table III. A typical example using values from test 83 (Table II) follows:

For anode heating

$$q = k\,(4.5 \pm 4.4\%)\,(555 \pm 2.7\%) \tag{18}$$
$$= 3.20 \pm 7.1\% = 3.20 \pm .227 \text{ kilowatts}$$

For cathode heating

$$q = k\,(7.1 \pm 2.8\%)\,(884 \pm 1.7\%) \tag{19}$$
$$= 8.05 \pm 4.5\% = 8.05 \pm .362 \text{ kilowatts}$$

For anode gas heating

$$q = k\,(12.6 \pm 1.6\%)\,(1494 \pm 2.0\%) \tag{20}$$
$$= 23.5 \pm 3.6\% = 23.5 \pm .845 \text{ kilowatts}$$

For radiation heating

$$q = k\,(1.9 \pm 10.5\%)\,(148 \pm 10.1\%) \tag{21}$$
$$= 0.33 \pm 21.5\% = 0.33 \pm .071 \text{ kilowatts}$$

For electrical power input

$$P = EI = (620 \pm 2.4\%)\,(104 \pm 3.8\%)$$
$$= 64.5 \pm 6.2\% = 64.5 \pm 4$$

For cathode gas heating

$$q = P - Q = 64.5 \pm 4.00 - 35.08 \pm 1.505 \tag{23}$$
$$= 29.42 \pm 5.5 \text{ kilowatts}$$
$$= 29.42 \pm 18.7\%$$

For anode enthalpy

$$H = k\frac{g}{m} = k\frac{23.5 \pm 3.6\%}{10.81 \pm 4\%} \qquad (24)$$

$$= 56{,}600 \pm 7.6\%$$

$$= 56{,}600 \pm 4300 \text{ BTU/lb}$$

For cathode enthalpy

$$H = k\frac{g}{m} = \frac{29.42 \pm 18.7\%}{21.6 \pm 8\%} \qquad (25)$$

$$= 35{,}100 \pm 26.7\%$$

$$= 35{,}100 \pm 9370 \text{ BTU/lb}$$

VI. Conclusions and Recommendations

This experiment sought information about reproduceability, efficiency, and enthalpy. These factors will be discussed in the order stated. Electrode loss mechanisms and operating techniques were covered completely in the preceding section. The chapter concludes with an optimization suggestion.

Reproduceability

The whirl stabilized hydrogen arc demonstrated questionable reproduceability especially below a current of ninety amperes. The characteristic could be changed very markedly according to the method of operation. In particular, different curves would obtain for a given pressure depending on whether the power was incremented upward or downward. Similarly, different curves would obtain according to whether the pressure was varied upward or downward.

This unusual aspect of operation must be studied more carefully since spectroscopic and photographic studies assume reproduceability. Subsequent investigation should first attempt to determine if any of the methods of operation result in a stable, reproduceable curve. If not, then instrumentation must be devised to measure the voltage - current characteristic of the column alone. The characteristic of the column has been measured previously and is known to be reproduceable. (Ref. 7; 898).

The discharge holes gradually enlarge by melting as tests proceed. This enlargement must have an effect on the radial and axial pressure

gradient and therefore on the arc channel diameter. The effect of this enlargement on reproduceability should be studied more carefully.

Efficiency

The arc efficiency for gas heating is excellent and with the modification of cathode hole diameter efficiency is expected to increase to above ninety percent. As mentioned before, this modification also increases cathode lifetime markedly. Even with the modification peak power is still limited by deterioration. One method for overcoming this limitation would be a movable rod type cathode located on the outside face of the present cathode and at right angles to the system axis. This rod would simply feed in automatically as it eroded.

Enthalpy

Gas enthalpy is not especially high because of the comparatively cold sheath of gas which surrounds the arc. The mixings of this cold gas with the hot plasma after discharge lowers the enthalpy considerably. Mr. Eric Soehngen of the Aeronautical Research Laboratory has suggested that this cold sheath of gas could be separated at the exit and recycled. The combination of this suggestion with the movable cathode rod and the modification of the cathode discharge hole diameter should result in a device of high enthalpy and long lifetime while retaining relatively high efficiency. Such an improvement might lead to an application as a heat transfer device. Electrode stabilization at the cathode side could also alleviate the reproduceability problem.

Bibliography

1. Cobb, C., and V. Blackman. Experimental Study of Spark Stabilization by a Gas Vortex. Plasmadyne Corporation Report No. TN 59-925. Washington: Air Force Office of Scientific Research, 1959.

2. Ecker, Gunter. Electrode Discharge Components of the Arc. ASTIA Document AD 217436. Bonn, Germany: United States Department of the Army, European Research Office, 1959.

3. Finkelnburg, W., and H. Maecker. Electric Arcs and Thermal Plasmas; in Handbuck der Physik, Volume 22, pp. 254-444. Berlin: Springer-Verlag, 1956.

4. Gardon, R. "An Instrument for the Direct Measurement of Intense Thermal Radiation". Reviews of Scientific Instruments, 24: 366-370 (1953).

5. Hodgman, C. D. Handbook of Chemistry and Physics. Cleveland, Ohio: The Chemical Rubber Publishing Co., 1960.

6. Penning, F. M. Electrical Discharges in Gases. New York: The Mac Millan Co., 1957.

7. Pfender, E., and W. Bez. "Report on a Pre-Discharge Arc", in Proceedings of the Fifth International Conference on Ionization Phenomena in Gases, Volume 1. Amsterdam, Netherlands: North Holland Publishing Co., 1962.

8. Thiene, P. G. Basic Study of Energy Exchange Process Between an Electric Arc and a Gas Flow. Plasmadyne Corporation Report No. 1264. Washington: Air Force Office of Scientific Research, 1961.

Appendix A

The Whirl Stabilized Arc in Nitrogen

Data for these results was obtained and reduced just as in the hydrogen experiment. As explained earlier, the nitrogen experiment was incomplete and of questionable validity. Some qualitative information may be obtainable, but a quantitative analysis is not possible. Trends may be misleading. The results presented here might be useful in designing another experiment using nitrogen; any further use is at the risk of the reader.

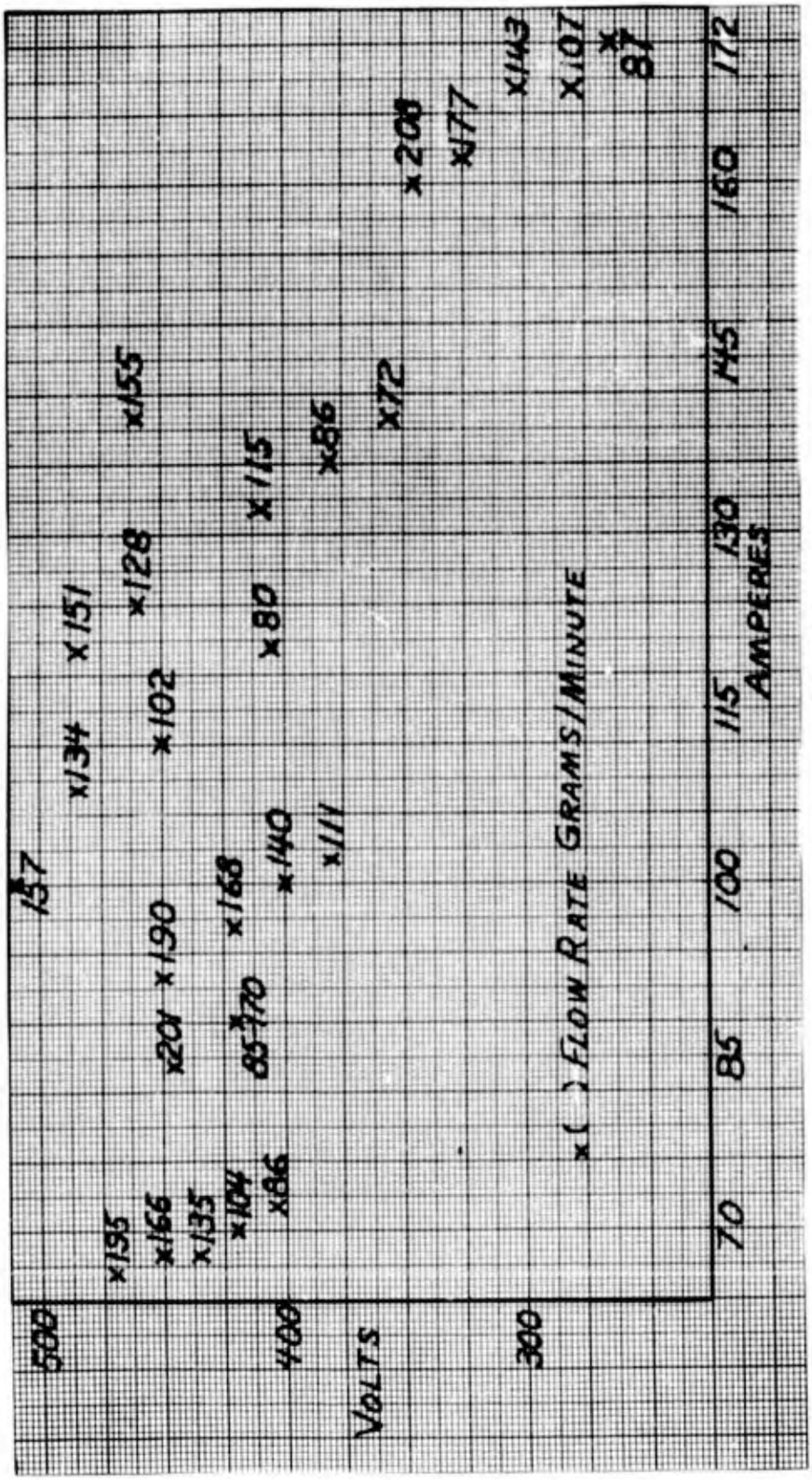

Figure A-1

Voltage Current Relation of the Nitrogen Arc

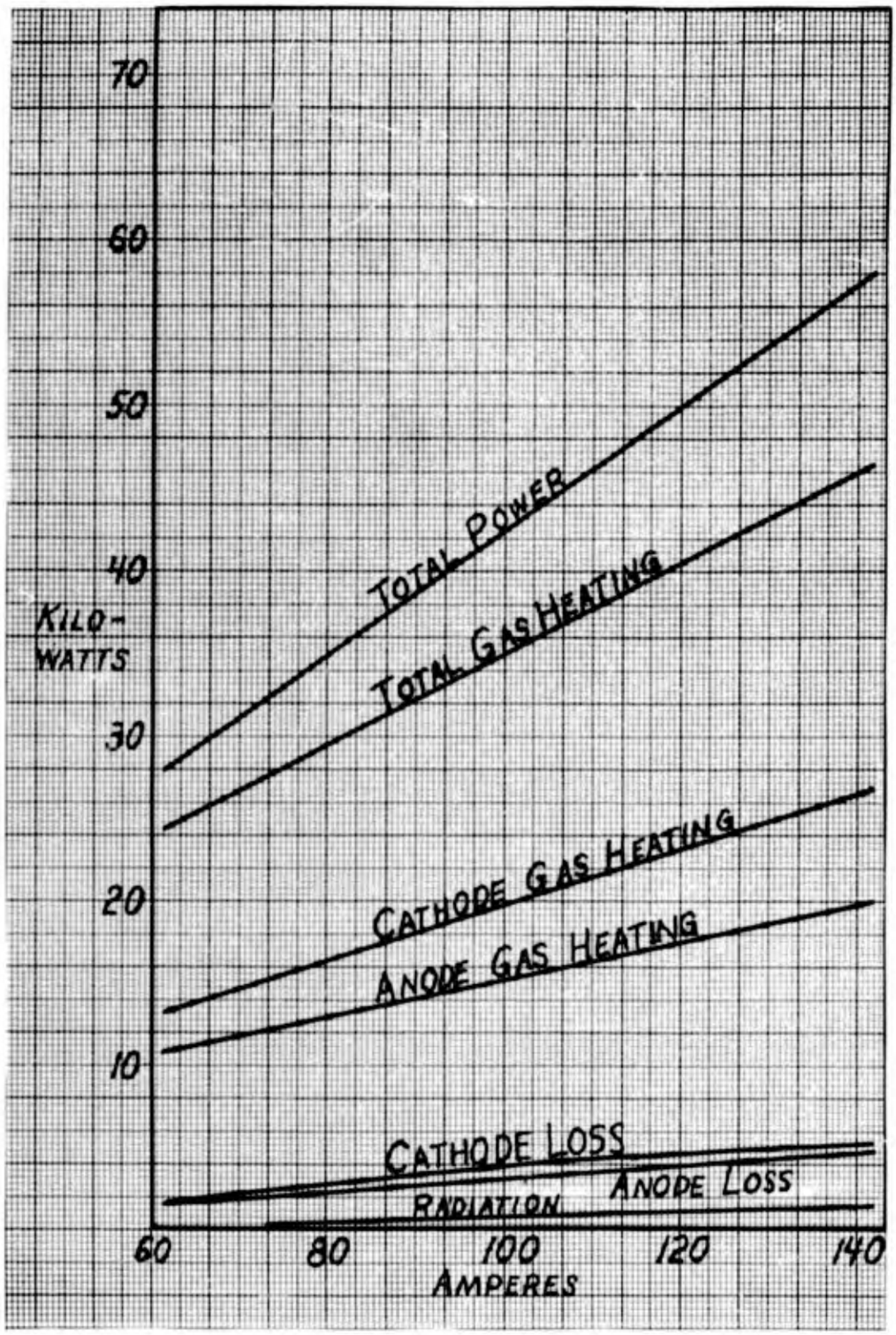

Figure A-2

Total Energy Balance of the Nitrogen Arc for a Flow Rate of about 140 Grams per Minute

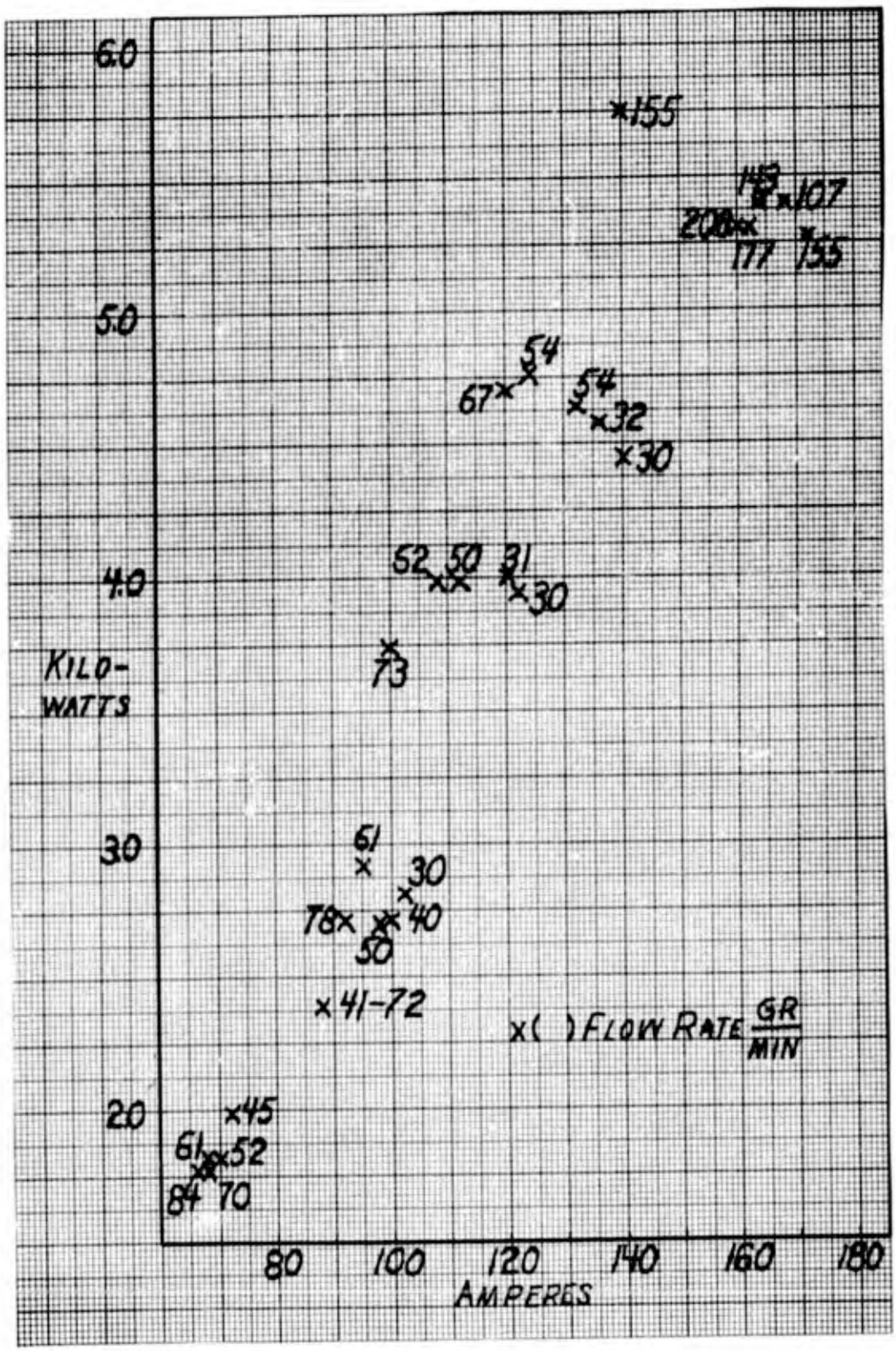

Figure A-3

Anode Losses as a Function of Current

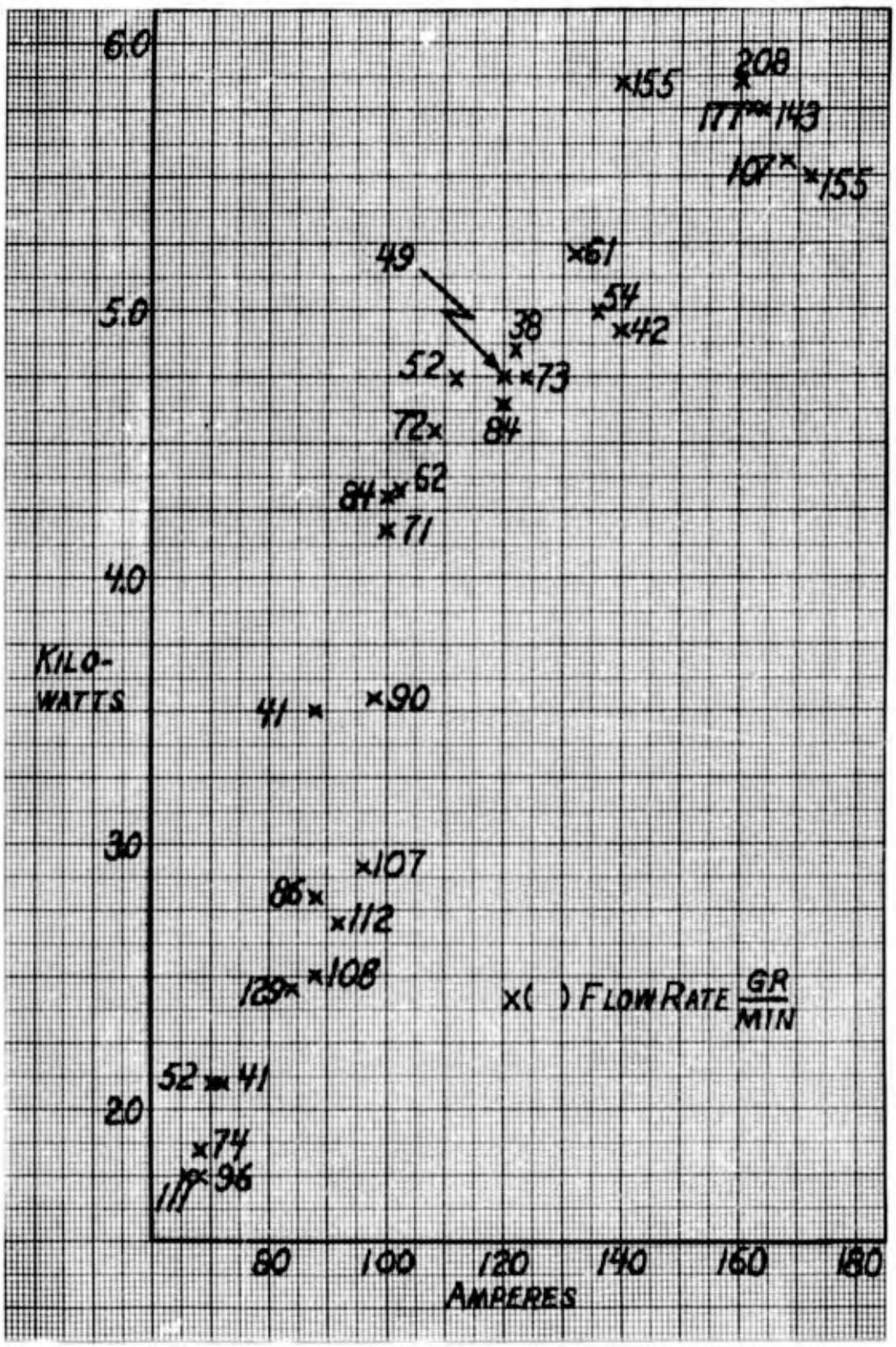

Figure A-4

Cathode Losses as a Function of Current

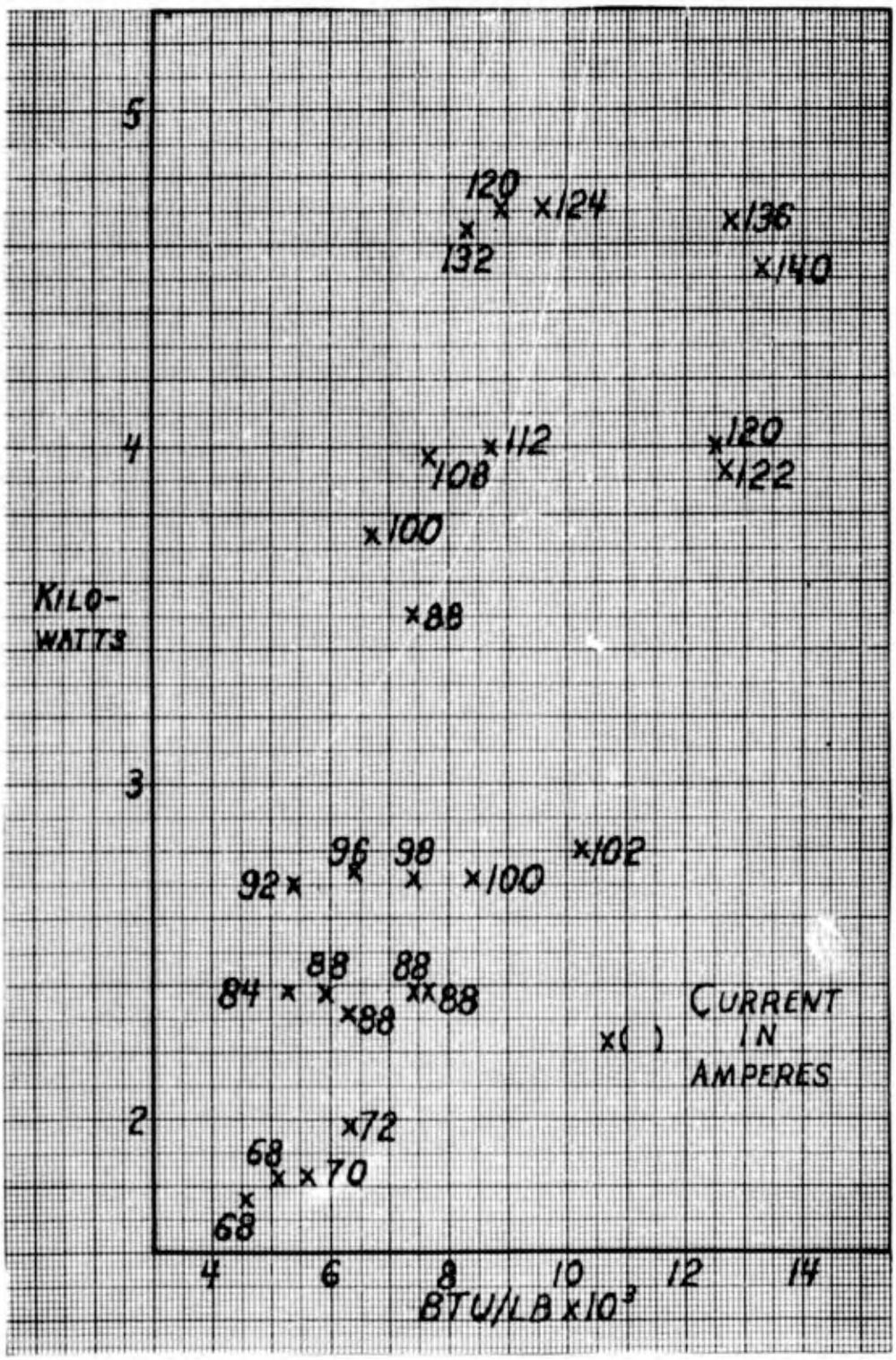

Figure A-5

Anode Losses as a Function of Enthalpy

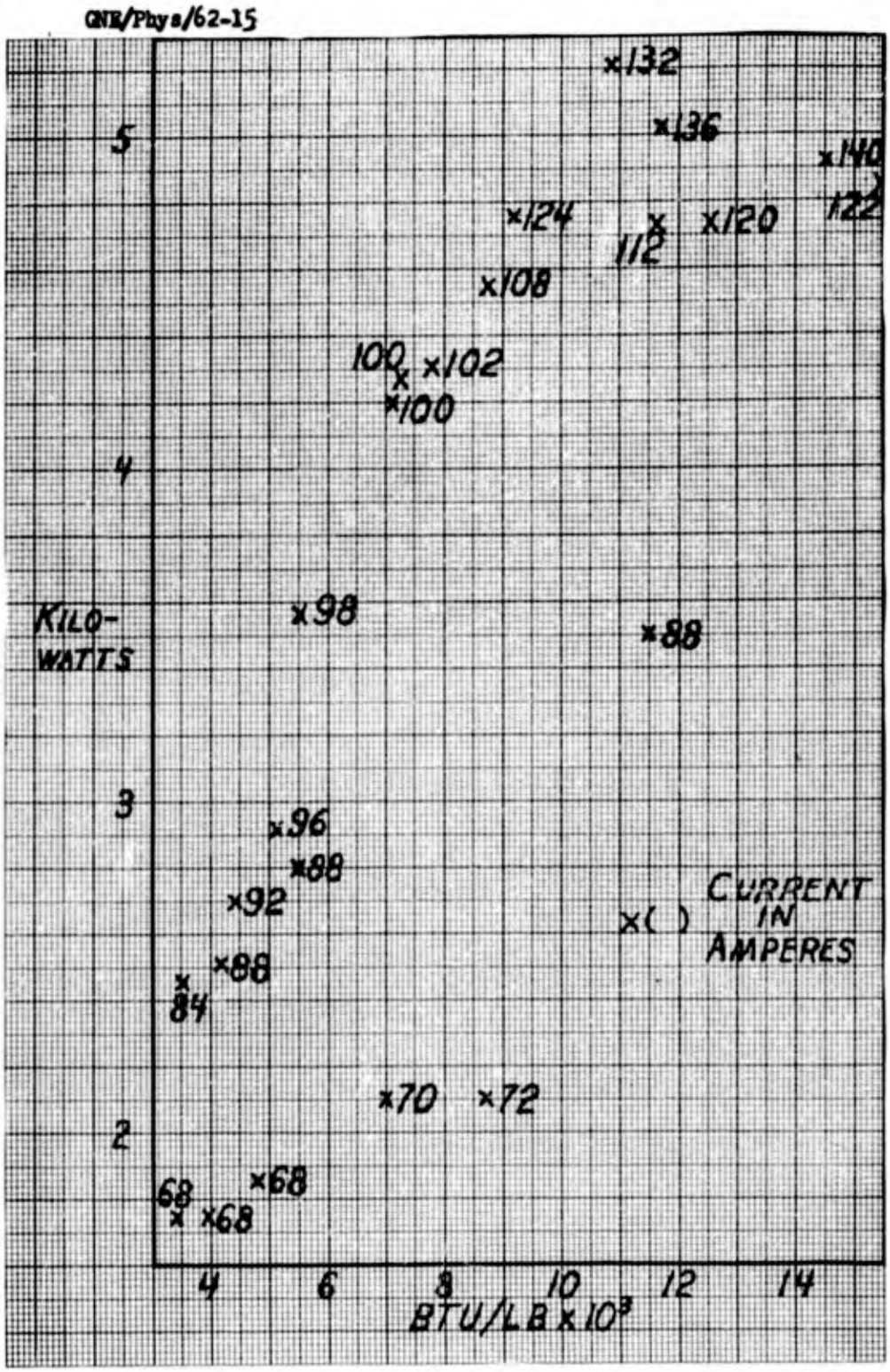

Figure 4-6

Cathode Losses as a Function of Enthalpy

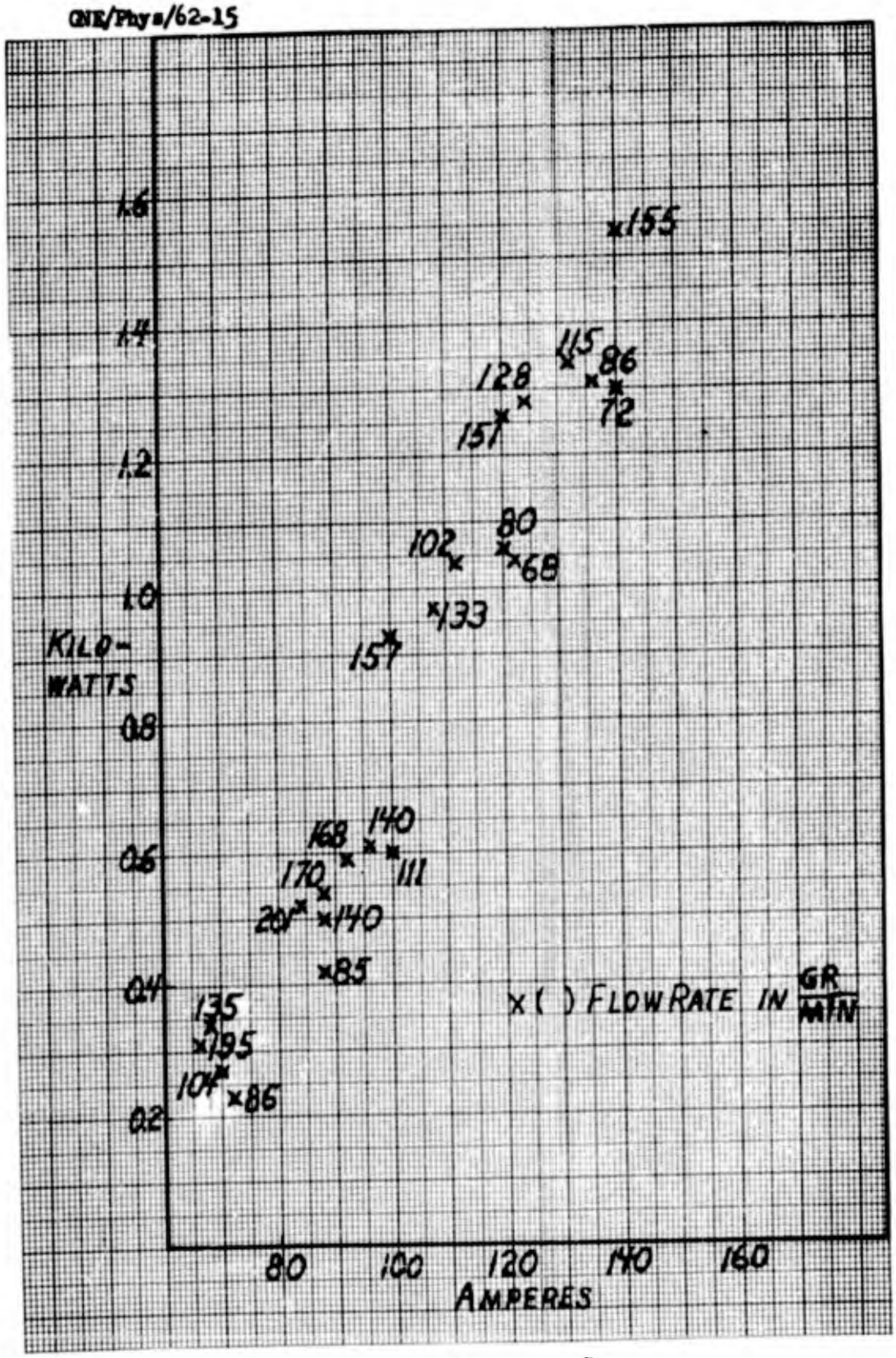

Figure 4-7

Radiated Power from the Nitrogen Arc
Radial Direction

Appendix B

List of Symbols

C_p - Specific heat at constant pressure

E - Supply voltage

F_a - Work function

H - Specific enthalpy

h - Film heat-transfer coefficient

I - Total current

I_+ - Positive ion current

I_- - Electron current

i_g - Enthalpy of the gas

i_w - Enthalpy of the wall

k - Correction factor for units

M - Mass flow

P - Total power

Q - Total power loss

q - Power loss for a given mechanism

S - Sub-total

T - Temperature

V_a - Anode fall

V_c - Cathode fall

V_i - Ionization potential

Vita

Thomas E. Reinhardt was born on [redacted], [redacted]. He graduated from [redacted] in 1950 and completed one term at Maryland State Teachers College, Towson, Maryland, in the fall of that year. He enlisted in the United States Army on 15 January 1951, and in June of 1952 entered the United States Military Academy from the Regular Army. He received a commission in the United States Air Force and a Bachelor of Science degree in Military Science on 9 June 1956. Prior to admission to the Institute of Technology, he served as a helicopter pilot in Air Rescue Service on Okinawa.

Permanent address: [redacted]

This thesis was typed by Mrs. Kay Bullock.

UNCLASSIFIED